Innovative Fresh Water Production Process for Fossil Fuel Plants

Annual Report

Reporting Period: 9/30/02-9/30/03

Principal Investigators: James F. Klausner and Renwei Mei
Graduate Students: Yi Li and Mohamed Darwish
Undergraduate Students: Diego Acevedo and Jessica Knight

September 2003

DOE Award Number **DE-FG26-O2NT41537**

University of Florida
Department of Mechanical and Aerospace Engineering
Gainesville, Florida 32611

Disclaimer*

Abstract

This report describes the annual progress made in the development and analysis of a Diffusion Driven Desalination (DDD) system, which is powered by the waste heat from low pressure condensing steam in power plants. The desalination is driven by water vapor saturating dry air flowing through a diffusion tower. Liquid water is condensed out of the air/vapor mixture in a direct contact condenser. A thermodynamic analysis demonstrates that the DDD process can yield a fresh water production efficiency of 4.5% based on a feed water inlet temperature of only 50° C. An example is discussed in which the DDD process utilizes waste heat from a 100 MW steam power plant to produce 1.51 million gallons of fresh water per day. The main focus of the initial development of the desalination process has been on the diffusion tower. A detailed mathematical model for the diffusion tower has been described, and its numerical implementation has been used to characterize its performance and provide guidance for design. The analysis has been used to design a laboratory scale diffusion tower, which has been thoroughly instrumented to allow detailed measurements of heat and mass transfer coefficient, as well as fresh water production efficiency. The experimental facility has been described in detail.

Table of Contents

1.0 Introduction

The continuous rise in the world population and the expansion of industrial facilities around the globe has placed a growing demand on the fresh water supply from natural resources (rivers, fresh water lakes, underground aquifers, and brackish wells). These resources have been steadily on the decline since the early 1950's. Therefore the need for new fresh water resources to balance the growing consumption rate has been a serious concern facing governments and world organizations for the past 50 years. It is widely recognized that a lack of sufficient fresh water can be destabilizing to governments.

In the United States there exists significant interest in developing clean-coal technologies for electricity generation to meet the growing electricity demand. Power generated from fossil fuels, especially coal, places a large demand on fresh water resources. Approximately 30 gallons of fresh water are required for every kWh of power produced from coal. This places fossil fired power plants in direct competition with processing industries and municipalities for fresh water resources that are on the decline. In some regions of the nation (Southeast and Southwest) fresh water is in such low supply, the environmental and regulatory concerns could be such to inhibit further development of clean-coal power generation technologies.

This report describes the annual research progress made toward the development of a diffusion driven desalination (DDD) process that may be used to produce large quantities of fresh water and replace cooling towers in existing or future fossil fired power plants. The tremendous advantage gained with this new technology is that the diffusion driven desalination process requires an energy input with very low thermodynamic availability. The energy to drive the DDD process would come from the low- pressure steam condensing in the main condenser. Therefore, the energy used to drive the desalination process is energy that would have otherwise been dissipated in the environment

The scope of this project includes analyzing the thermodynamic parameters governing the DDD process, developing an analytical heat and mass transfer model that may be used to design and optimize an operational DDD facility, fabricating a laboratory scale DDD processing plant, conduct detailed heat, mass, and momentum transfer experimental studies using the experimental DDD facility, and use the experimental results to validate the design model. At the completion of the project, sufficient design and analysis tools should be developed to fabricate an industrial scale DDD processing facility with a high degree of confidence. The contents of this report relate the progress made during the first year of research.

The DDD process is a thermal process that operates using waste heat, and it provides potential to produce inexpensive fresh water. A very interesting application for the DDD process is to operate in conjunction with an existing process that produces large amounts of waste heat and is located in the vicinity of an ocean or sea. One such potential benefactor of the DDD process is the electric utility industry. Conventional steam driven power plants dump a considerable amount of energy to the environment via cooling water that is used to condense low pressure steam within the main condenser. Typically this cooling water is either discharged back to its original source or it is sent to a cooling tower, where the thermal energy is discharged to the atmosphere. Instead of

dumping the thermal energy to the environment, the DDD process provides a means for putting the discarded thermal energy to work to produce fresh water. Of course this application is limited to power producing facilities sited along the coastline.

As an example, consider that a 100 MW steam driven power plant operating with 2" Hg vacuum in the main condenser would require 1100 kg/s of cooling water discharging the main condenser at 50° C. If retrofitted with a DDD plant, there is potential to produce as much as 1.5 million gallons of fresh water over a 24 hour period. The production rate would increase with a higher cooling water discharge temperature from the main condenser. The electrical cost of pumping air and water through the diffusion tower is only 0.002 kW-h/kg or 40 cents per 1000 gallons of fresh water production. In comparison, the energy consumption of multistage flash evaporation (MSF) is typically 0.025 kW-h/kg, while that of reverse osmosis (RO) is typically 0.007 kW-h/kg. The low temperature operation of the DDD process is economically advantageous in that inexpensive materials may be used to construct a facility.

1.1 Humidification Dehumidification Processes

A desalination technology that has drawn interest over the past two decades is referred to as Humidification Dehumidification (HDH). This processes operates on the principle of mass diffusion and utilizes dry air to evaporate saline water, thus humidifying the air. Fresh water is produced by condensing out the water vapor, which results in dehumidification of the air. A significant advantage of this type of technology is that it provides a means for low pressure, low temperature desalination and can potentially be very energy efficient. Bourouni et al., Al-Hallaj et al., and Assouad et al. [1-3] respectively reported the operation of HDH units in Tunisia, Jordan, and Egypt. An excellent comprehensive review of the HDH process is provided by Al-Hallaj and Selman [4]. It was concluded that although the HDH process is very energy efficient, it is not currently cost competitive with reverse osmosis (RO) and multistage flash evaporation (MSF). There are four primary reasons for the higher costs associated with the HDH process:

1) The HDH process is typically applied to low production rates and economies of scale cannot be realized in construction.
2) Typically natural draft is relied upon, which results in low heat and mass transfer coefficients and a larger surface area humidifier.
3) Solar heating is typically utilized, which requires a larger land footprint to site the plant, and it constrains the production capacity.
4) Film condensation over tubes is typically used, which is extremely inefficient when non-condensable gases are present. Thus a much larger condenser area is required for a given production rate.

Therefore, an economically feasible diffusion driven distillation process must overcome these shortcomings.

1.2 DDD Process Description

A simplified schematic diagram of the DDD process and system are shown in Figure 1. The process is described here. A main feed pump (a) draws water from a large body of seawater. The suction for the pump draws water near the surface in order to take advantage of the fact that large bodies of water absorb solar radiation, and due to thermal

stratification, the warmer water is in the vicinity of the surface, while cooler water resides at larger depths beneath the surface. The surface water is pumped through the main feed water heater (b). The amount of heat required depends on the main feed water mass flow rate and desired production rate. The required output temperature from the heater is relatively low, and therefore the required heat input can be provided by a variety of sources, depending on the available resources. It is envisioned that heat can be provided from low pressure condensing steam in a power plant, exhaust from a combustion engine, waste heat from an oil refinery, or other waste heat sources. After the feed water is heated in the main heater, it is sprayed into the top of the diffusion tower (c). The diffusion tower is one of the most important piece of equipment in the process, and the degree to which an operational DDD process follows theoretically predicted trends depends on an appropriately designed diffusion tower. On the bottom of the diffusion tower, low humidity air is pumped in using a forced draft blower (d). The water falls concurrently to the airflow through the diffusion tower by the action of gravity. The diffusion tower is packed with very high surface area packing material. As water flows through the diffusion tower, a thin film of water forms over the packing material and contacts the air flowing upward through the tower. As dictated by Fick's law and the conservation of mass, momentum, and energy, liquid water will evaporate and diffuse into the air, while air will diffuse into the water, due to concentration gradients. The diffusion tower should be designed such that the air/vapor mixture leaving the diffusion tower should be fully saturated. The purpose of heating the water prior to entering the diffusion tower is that the rate of diffusion and the exit humidity ratio increase with increasing temperature, thus yielding greater production. The water not evaporated in the diffusion tower, will be collected at the bottom and removed with a brine pump (e). The brine will be discharged.

The air entering the diffusion tower will be dried in the direct contact condenser (g). The saturated air/vapor mixture leaving the diffusion tower is drawn into the direct contact condenser with a forced draft blower (f), where the water vapor is condensed into fresh liquid water that is collected in the sump of the condenser. Another very important component of the DDD process is the condenser. The difficulty that arises is that film condensation heat transfer is tremendously degraded in the presence of non-condensable gas. The same difficulty was faced in the design and development of condensers for OTEC (Ocean Thermal Energy Conversion) applications. In order to overcome this problem Bharathan et al. [5] describe the use of direct-contact heat exchangers. In their excellent report, they have developed models for simulating the heat transfer and have validated the models with careful experimentation. For the present application involving desalination, the warm fresh water discharging the direct contact heat exchanger will be chilled in a conventional shell-and-tube heat exchanger (h) using saline cooling water. The cooling water is drawn from a large depth to take advantage of the thermal stratification in large bodies of water. A portion of the chilled fresh water will be directed back to the direct contact heat exchanger to condense the water vapor from the air/vapor mixture discharging from the diffusion tower. The rest of the fresh water is make-up water. The direct contact condenser approach is best suited for the DDD process.

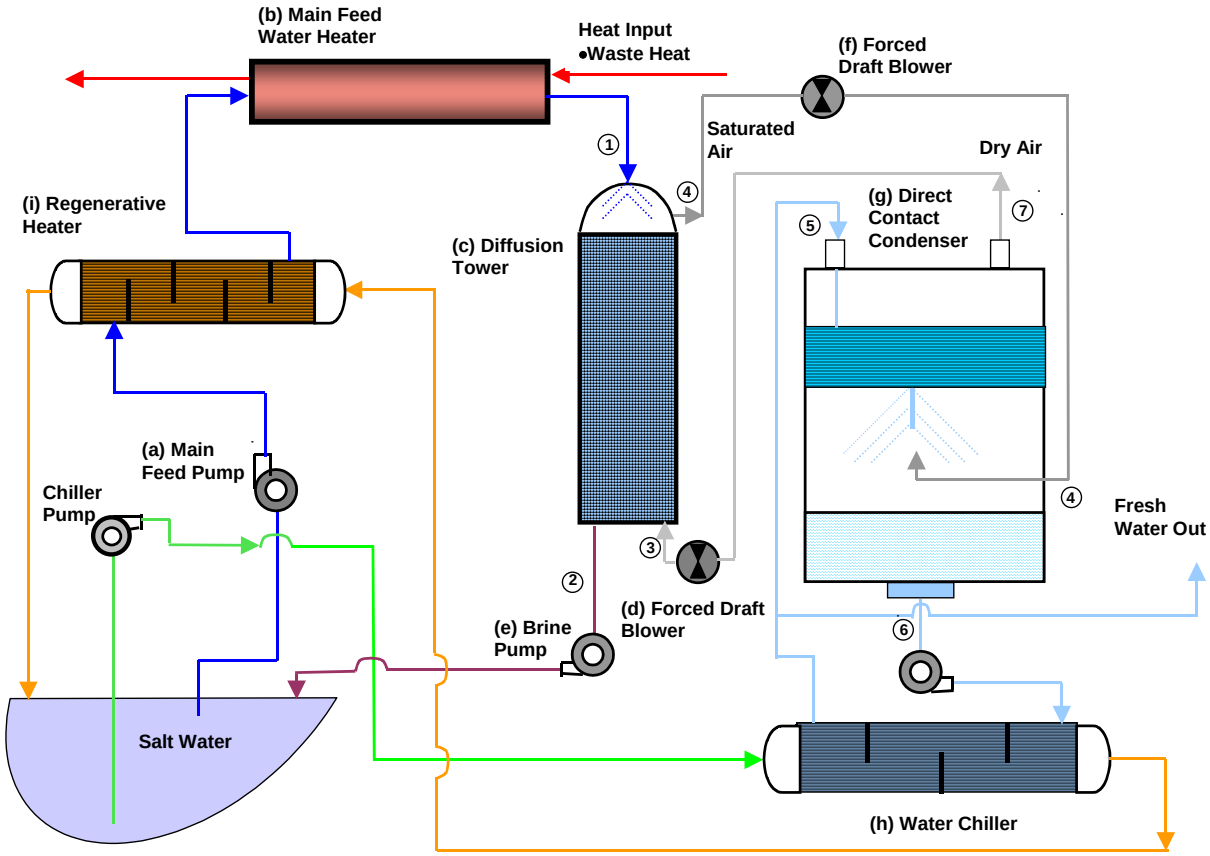

Figure 1 Flow Diagram of Diffusion Driven Desalination Process

The diffusion driven desalination process has the following advantages compared with other humidification dehumidification processes:

1) The DDD process utilizes thermal stratification in the seawater to provide improved performance. In fact, the DDD process can produce fresh water without any heating by utilizing the seawater thermal stratification.
2) The thermal energy required for the DDD process may be entirely driven by waste heat, and there is no need for solar heating or solar panels. This helps keep the DDD plant compact, which translates to reduced cost. Solar heating requires a substantial amount of un-shaded land to produce a meaningful quantity of water. This may be suitable for desert locations but would be prohibitively expensive to use in populated coastline regions. The DDD process recommends using whatever heat source is best suited for the region requiring fresh water production. The DDD process is very well suited to be integrated with steam power plants, and use the waste heat coming from these plants.

3) In the DDD process the evaporation occurs in a forced draft packed bed diffusion tower as opposed to a natural draft humidifier. The diffusion tower is packed with low pressure-drop, high surface area packing material, and provides significantly greater surface area. This is very important because the rate of water evaporation is directly proportional to the liquid/vapor surface area available. In addition, the forced draft provides for high heat and mass transfer coefficients. Thus, a diffusion tower is capable of high production rates in a very compact unit. Since the unit is compact, the capital cost will be minimized. The price paid in using forced draft is the pumping power required to pump the fluids through the system, but as will be demonstrated this cost is low compared with RO and MSF.
4) The DDD process uses a direct contact condenser to extract fresh water from the air/water vapor mixture. This type of condenser is significantly more efficient than a conventional tube condenser, as is used with the HDH process. Thus, the condenser will be considerably more compact for a given design production rate. This also adds to cost reduction.
5) The diffusion tower and direct contact condenser can accommodate very large flow rates, and thus economies of scale can be taken advantage of to produce large production rates.
6) No exotic components are required to manufacture a DDD plant. All of the components required to fabricate a DDD plant are manufactured in bulk and are readily available from different suppliers. This fact also translates to reduced cost.

2.0 Thermodynamic Analysis of the DDD Process

In order to explore the performance and parametric bounds of the Diffusion Driven Desalination process, a thermodynamic cycle analysis has been performed. In performing the analysis the following assumptions have been made,

1. The process operates at steady-state conditions,
2. There are no energy losses to the environment from the heat and mass transfer equipment,
3. Air and water vapor may be treated as a perfect gas,
4. Changes in kinetic and potential energy are relatively small,
5. The pumping power is neglected in the energy balance (estimating the required pumping power would require significant details regarding the construction of the diffusion tower and heat transfer equipment; these are beyond the scope of the current analysis).

In the analysis, the temperature of the feed water drawn into the main feed pump is fixed at 27° C. It is assumed that a large supply of cool water will be available at a sink temperature, T_L, of 15° C. The condensate in the direct contact condenser will be chilled and a portion of it re-circulated. To avoid providing specifics on the heat transfer equipment, it is assumed that the heat transfer effectiveness in the chiller and condenser is unity, in which case $T_L=T_5=T_7=15°$ C. The temperature of the feed water leaving the main heater is the high temperature in the system, $T_H=T_1$, and is a primary controlling variable for the process. Different performance curves will be shown for a variable T_H.

The air/vapor mixture leaving the diffusion tower is assumed to be fully saturated (relative humidity of unity), and due to heat transfer limitations, its maximum temperature will be taken to be that of the feed water entering the diffusion tower ($T_4 \leq T_1$).

The main purpose of this analysis is to explore the performance bounds of the DDD process. However, specification of the system operating variables is not arbitrary. Namely there are two constraints that must be satisfied,

1. The brine temperature leaving the diffusion tower must not be lower than the air inlet temperature (T_2>15° C), so that the air can always absorb heat from the brine during the humidification process through the diffusion tower, and
2. The net entropy generation in the diffusion tower must be positive.

These constraints govern the parametric bounds for the diffusion tower operation. While the first constraint is initially obvious, the second constraint is simply a restatement of the second law of thermodynamics for the present adiabatic system (diffusion tower). The control volume formulation of the second law of thermodynamics for an open system is expressed as,

$$\frac{Ds}{Dt} = \frac{\partial}{\partial t}\int_V \rho s dV + \oint_A \rho s \vec{v} \cdot d\vec{A} \geq \oint_A \frac{1}{T}\frac{\dot{Q}}{A} dA, \qquad \textbf{(1)}$$

where V denotes the control volume, A is the control surface, and s is the entropy per unit mass. Assuming steady state processing of fresh water, the adiabatic diffusion tower assumption leads to,

$$\dot{s} = \frac{Ds}{Dt} = \oint_A \rho s \vec{v} \cdot d\vec{A} \geq 0, \qquad \textbf{(2)}$$

and

$$\dot{s} = m_{l2}s_{l2} + m_a s_{a4} + m_{v4}s_{v4} - m_{l1}s_{l1} - m_a s_{a3} - m_{v3}s_{v3} \qquad \textbf{(3)}$$

where m denotes the mass flow rate and the subscripts l, a, and v respectively refer to the liquid, air, and vapor phases. The numerical subscripts denote that the property is evaluated at the state corresponding to the position in the process as shown schematically in Figure 1. Conservation of mass dictates that,

$$\frac{m_{l2}}{m_a} = \frac{m_{l1}}{m_a} - (\omega_4 - \omega_3). \qquad \textbf{(4)}$$

The rate of entropy generation in the diffusion tower per rate of air flow, which must be positive, is obtained from rearranging Eq. (3) and combining with Eq. (4) as,

$$\frac{\dot{s}}{m_a} = \left[\frac{m_{l1}}{m_a} - (\omega_4 - \omega_3)\right] s_{l2} + C_{pa}\ln\left(\frac{T_4}{T_3}\right) - R_a \ln\left(\frac{P_{a4}}{P_{a3}}\right) + \omega_4 s_{v4} - \omega_3 s_{v3} - \frac{m_{l1}}{m_a} s_{l1}, \qquad \textbf{(5)}$$

where ω is the humidity ratio, C_p is the specific heat, R is the engineering gas constant, and P_a is the partial pressure of air.

The control volume formulation of energy conservation applied to the adiabatic diffusion tower leads to,

$$m_{l1}h_{l1} + m_a h_{a3} + m_{v3}h_{v3} - m_{l2}h_{l2} - m_a h_{a4} - m_{v4}h_{v4} = 0 \qquad \textbf{(6)}$$

where h denotes the enthalpy. The enthalpy of the brine exiting the diffusion tower is obtained from Eqs. (6) and (4) as,

$$h_{l2}(T_2) = \frac{\frac{m_{l1}}{m_a} h_{l1} - C_{pa}(T_4 - T_3) + \omega_3 h_{v3} - \omega_4 h_{v4}}{\frac{m_{l1}}{m_a} - (\omega_4 - \omega_3)}, \quad \textbf{(7)}$$

and the brine temperature (T_2) is evaluated from the enthalpy. The air to feed water mass flow ratio through the diffusion tower, m_a/m_{l1}, is another controlling variable in the analysis. For all computations the feed water mass flow rate will be fixed at 100 kg/s while the air mass flow rate will be varied.

The humidity ratio entering the diffusion tower, ω_3, is determined by recognizing that it is the same as the humidity ratio exiting the condenser, where T_7 is 15 °C.

The first case considered is where there is no heating in the main heater. The desalination process is entirely driven by the difference in temperature of the feed water drawn at shallow depths and the cooling water drawn at more substantial depth. In this case, T_H=27°C, T_L=15°C. Figure 2 shows the rate of entropy generation within the diffusion tower and the brine temperature exiting the diffusion tower for a locus of possible operating conditions. Here it is observed that the second law of thermodynamics is always satisfied for the entire parametric range considered, but there is a maximum entropy generation point with different air to feed water mass flow ratio. Figure 3 shows the brine temperature (T_2) exiting the diffusion tower as a function of the exit air temperature from the diffusion tower (T_4) for the same locus of operating conditions as in Figure 2. It clearly shows that the exit brine temperature decreases as the exit air temperature increases, and the rate of brine temperature decrease increases with increasing the air to feed water mass flow ratio. Because it is assumed the exit air is saturated, it is advantageous to have as high an air temperature leaving the diffusion tower so that the humidity ratio and fresh water production rate are as high as possible. For this case the exit air temperature is constrained by the inlet feed water temperature (T_1) when the air to feed water mass flow ratio is lower than unity. When the air to feed water mass flow ratio exceeds unity, the exit air temperature is limited by the fact that the brine exit temperature must be higher than the air inlet temperature. Figure 4 shows the fresh water to the feed water mass flow ratio as a function of the exit air temperature for different air to feed water mass flow ratios. Clearly, the production rate increases with increasing exit air temperature under the same air to feed water mass flow ratio, meanwhile the production rate grows with increasing the air to feed water mass flow ratios under the same exit air temperature. However, both these parameters are constrained because the exit air temperature must not exceed T_H, and for the case of no heating of the feed water (T_H=27° C, T_L=15° C), the maximum fresh water production efficiency (m_{fw}/m_{l1}) is approximately 0.014.

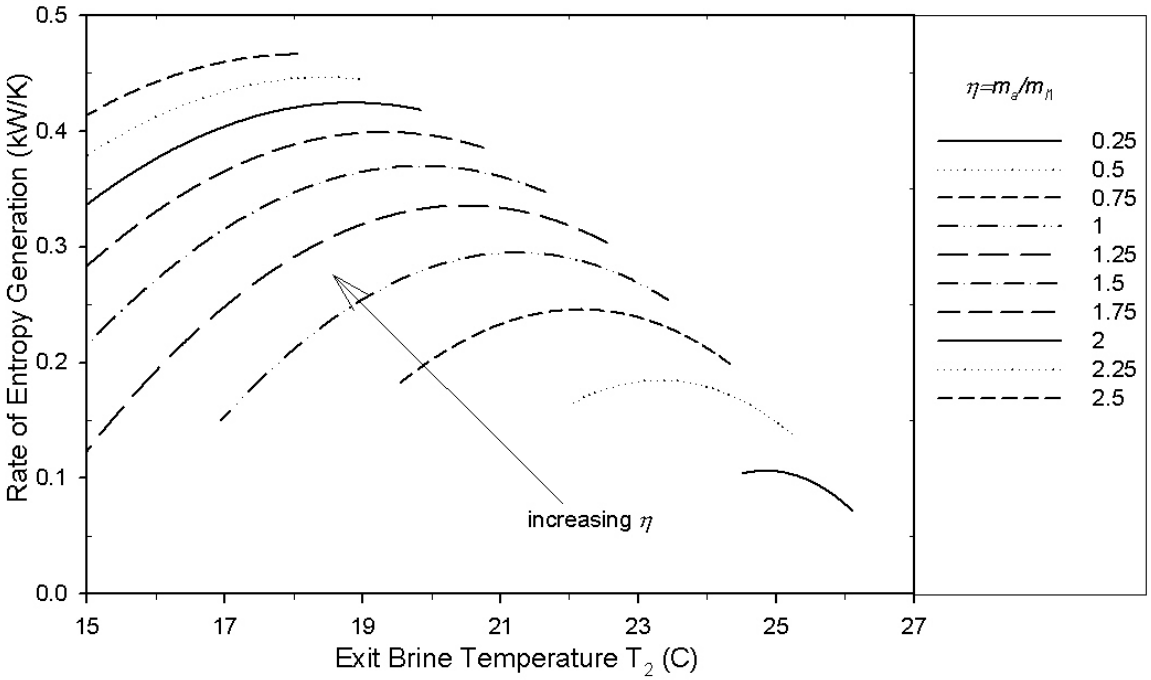

Figure 2 Rate of entropy generation for different exit brine temperature, T_H=27°C

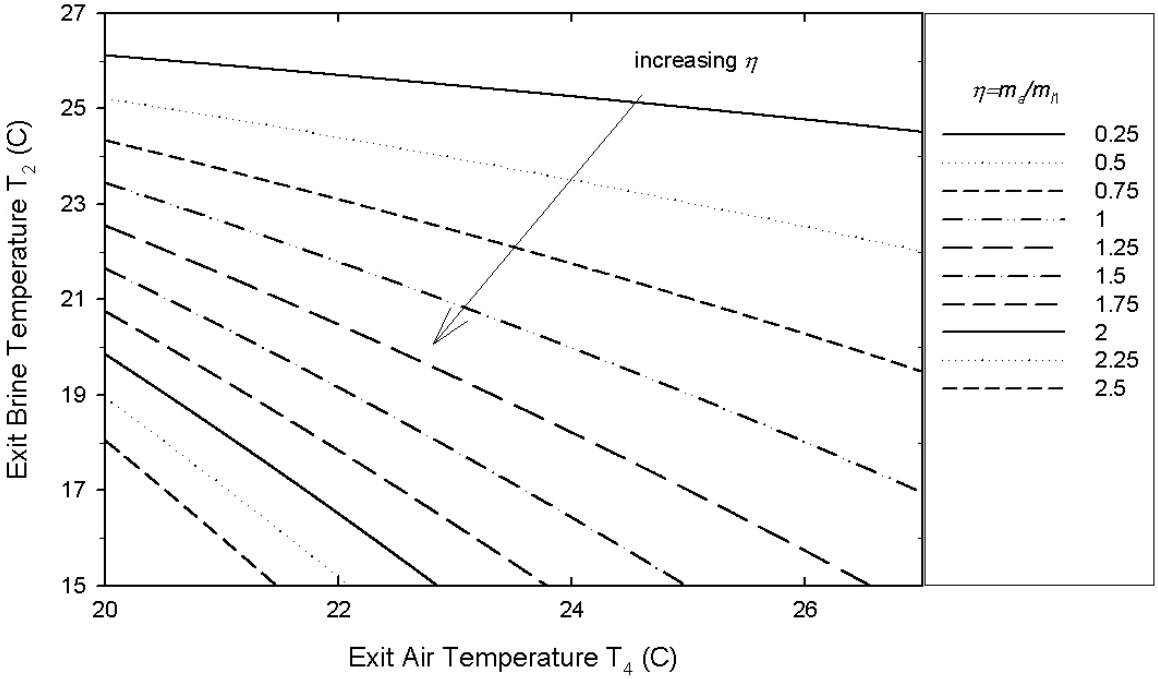

Figure 3 Variation of exit brine temperature with exit air temperature, T_H=27°C

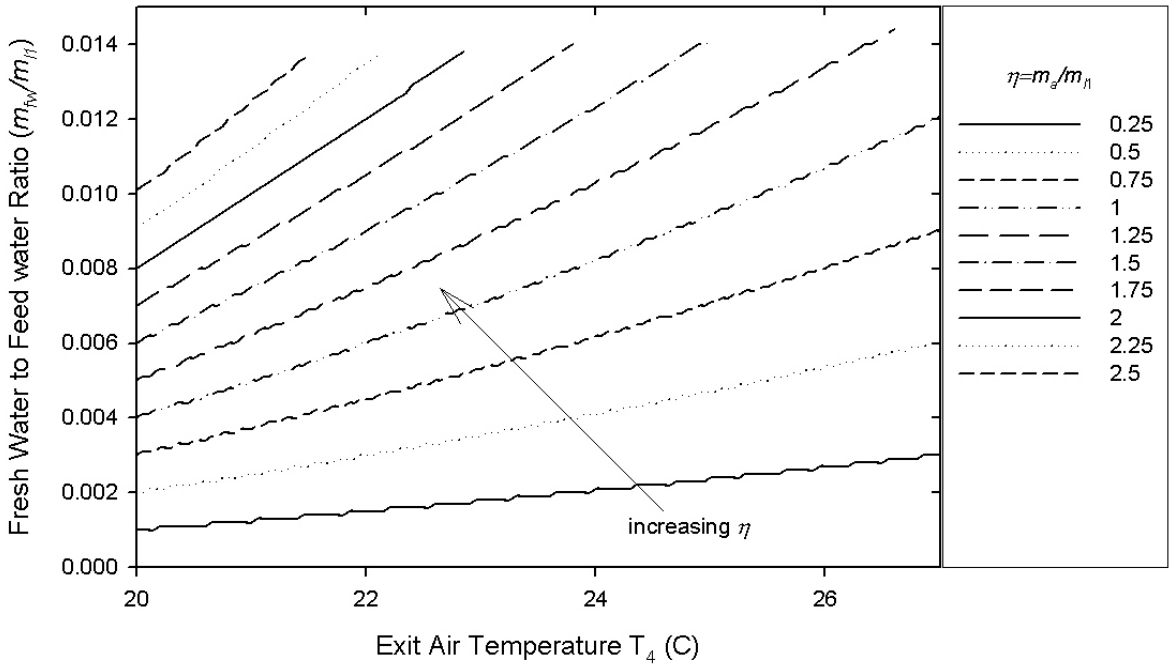

Figure 4 Fresh water production efficiency, T_H=27° C

The next cases considered are where the diffusion tower inlet water temperatures are 50° C and 80° C. Figures 5 and 6 show the rate of entropy generation in the diffusion tower for T_H=50° C and 80° C, respectively. Again the second law of thermodynamics is satisfied for the entire parametric range considered. The entropy generation tends to be lower for lower air to feed water flow ratios under the same exit brine temperature and has the maximum value with a certain exit brine temperature under the same air to feed water mass flow ratio. At higher air to feed water flow ratios, the constraint is that the brine temperature must be higher than the air inlet temperature. Figure 7 shows the range of possible exit brine temperatures and exit air temperatures for different air to feed water flow ratios when the diffusion tower inlet water temperature is 50° C. Figure 8 shows the range of temperatures when the diffusion tower inlet water temperature is 80° C. The maximum fresh water production will occur with as high an exit air temperature as possible. For the energy balance on the diffusion tower, the exit brine temperature decreases with increasing exit air temperature and the rate of brine temperature decrease increases with increasing the air to feed water mass flow ratio. In contrast to the case with no heating, the exit air temperature is primarily constrained by the fact that the brine cannot be cooler than the inlet air, especially at higher air to feed water flow ratios. At very low air to feed water flow ratios, the exit air temperature is constrained by the inlet water temperature when T_H is 50° C, meanwhile it is constrained by the fact that entropy generation must be positive when T_H is 80° C.

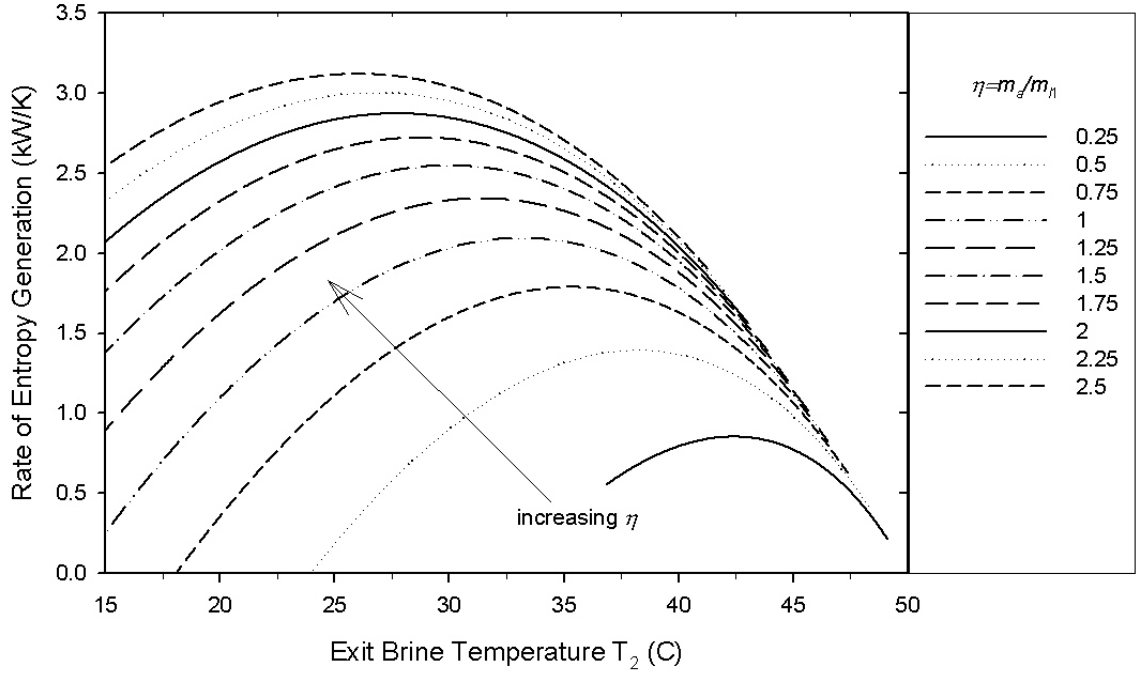

Figure 5 Rate of entropy generation for different exit brine temperature, T_H=50° C

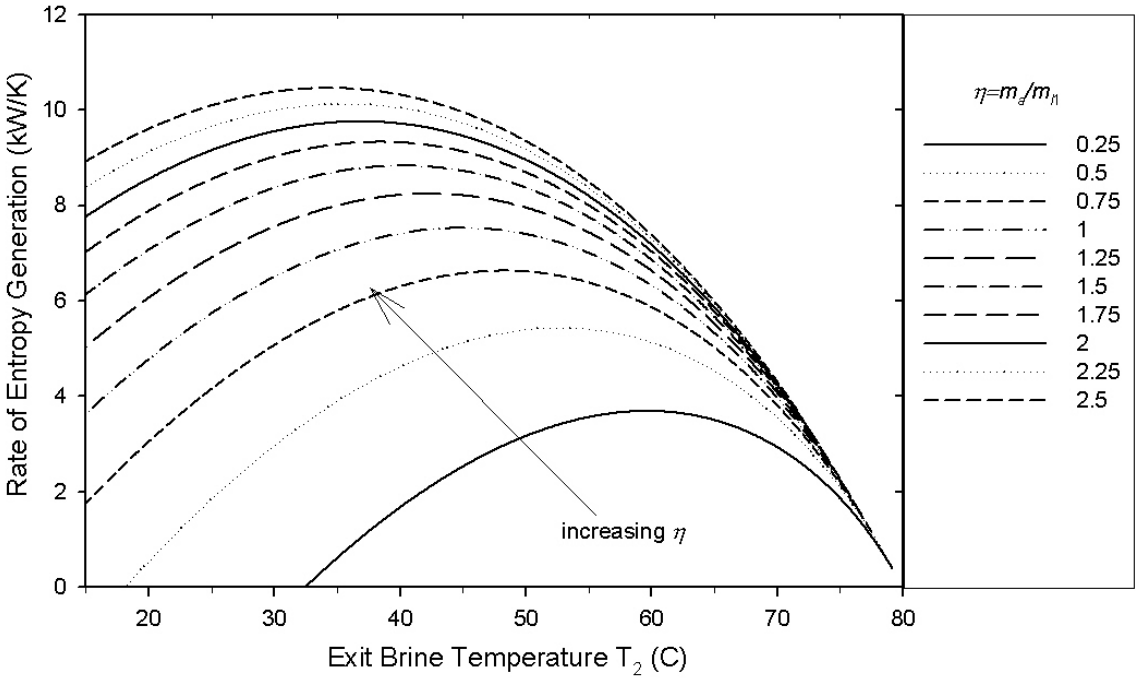

Figure 6 Rate of entropy generation for different exit brine temperature, T_H=80° C

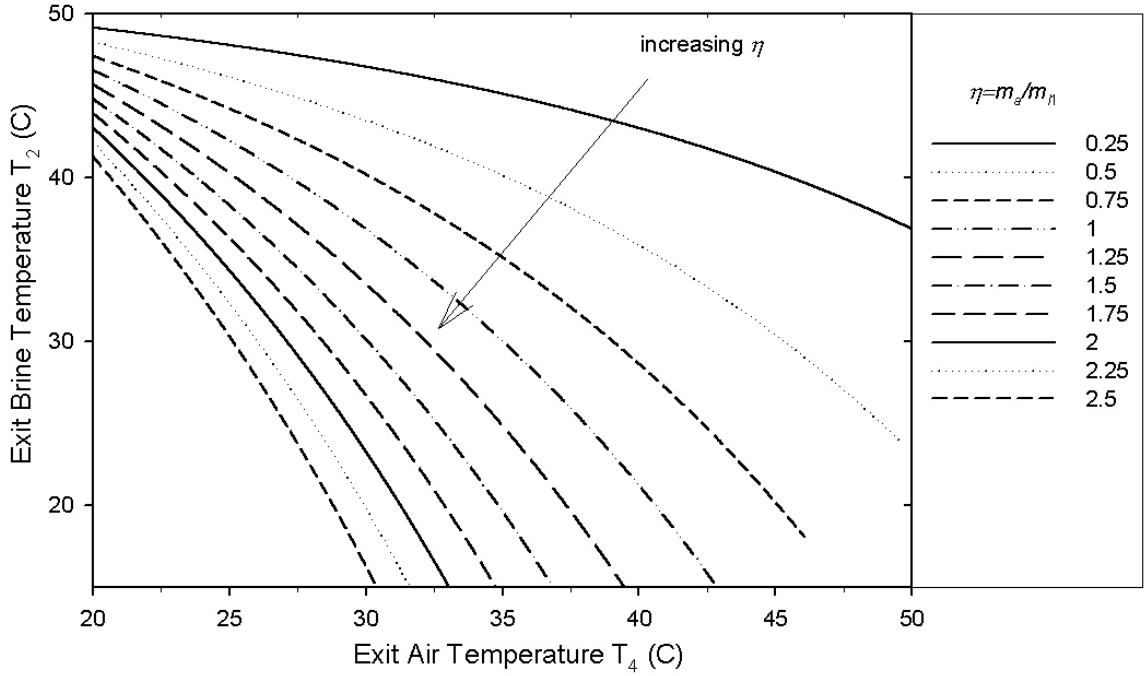

Figure 7 Variation of exit brine temperature with exit air temperature, T_H=50° C

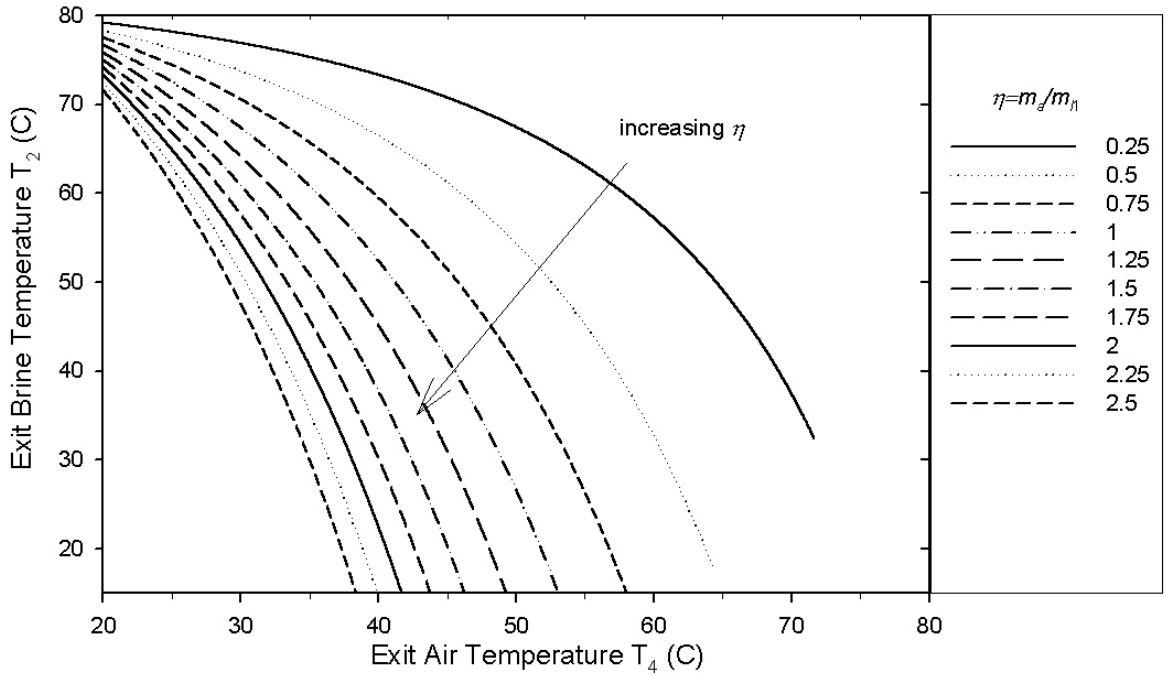

Figure 8 Variation of exit brine temperature with exit air temperature, T_H=80° C

For respective diffusion tower inlet water temperatures of 50° C and 80° C, Figures 9 and 10 show the ratio of fresh water production efficiency as a function of the exit air temperature for different air to feed water flow ratios. It is observed that the fresh water production efficiency increases with increasing exit air temperature and increasing air to feed water flow ratio. The maximum fresh water production efficiency for T_H=50° C is approximately 0.045 when air to feed water flow ratio is 1, while that for T_H=80° C is approximately 0.1 when air to feed water flow ratio is 0.75. Therefore, one advantage of increasing the diffusion tower inlet water temperature is that the fresh water production efficiency increases.

For respective diffusion tower inlet water temperatures of 50° C and 80° C, Figures 11 and 12 show the thermal energy consumed per unit of fresh water production as a function of exit air temperature for different air to feed water flow ratios over the entire parameter space considered. Although, details of the low energy consumption regime are difficult to discern, it is interesting to observe that increasing both the exit air temperature and the air to feed water mass flow ratio results in a reduced rate of energy consumption. In order to explore the lower energy consumption regime Figures 13 has been prepared for diffusion tower inlet water temperatures of 50° C, 60° C, 70° C and 80° C, respectively. It shows the lowest energy consumed per unit of fresh water production as a function of different air to feed water flow ratios for different T_H. Obviously, there exists a minimum at a certain air to feed water mass flow ratio for every T_H. For T_H=50°C the minimum rate of energy consumption is about 0.56 kW-h/kg_{fw} when the air to water mass flow ratio is 1, while that for T_H=80° C is approximately 0.65 kWh/kg_{fw} when the air to water mass flow ratio is 0.5. The results also indicate that the minimum rate of energy consumption will occur with lower air to feed water mass flow ratio when T_H is higher. In this analysis the energy consumption due to pumping is neglected, however, it is another important part of the energy consumption required for the system. Therefore, it is expected that in actual practice there exists some minimum energy consumption associated with a specific air to feed water mass flow ratio. The inclusion of the pumping power in the overall analysis is the subject of the design analysis in the next section.

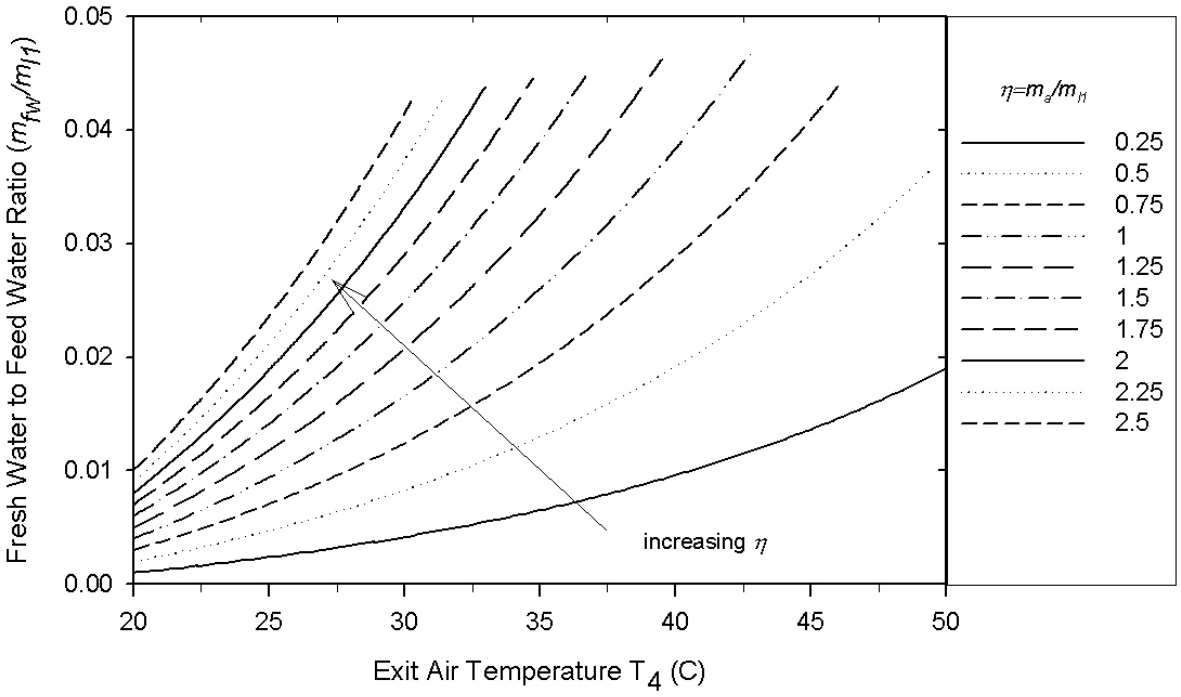

Figure 9 Fresh water production efficiency, T_H=50° C

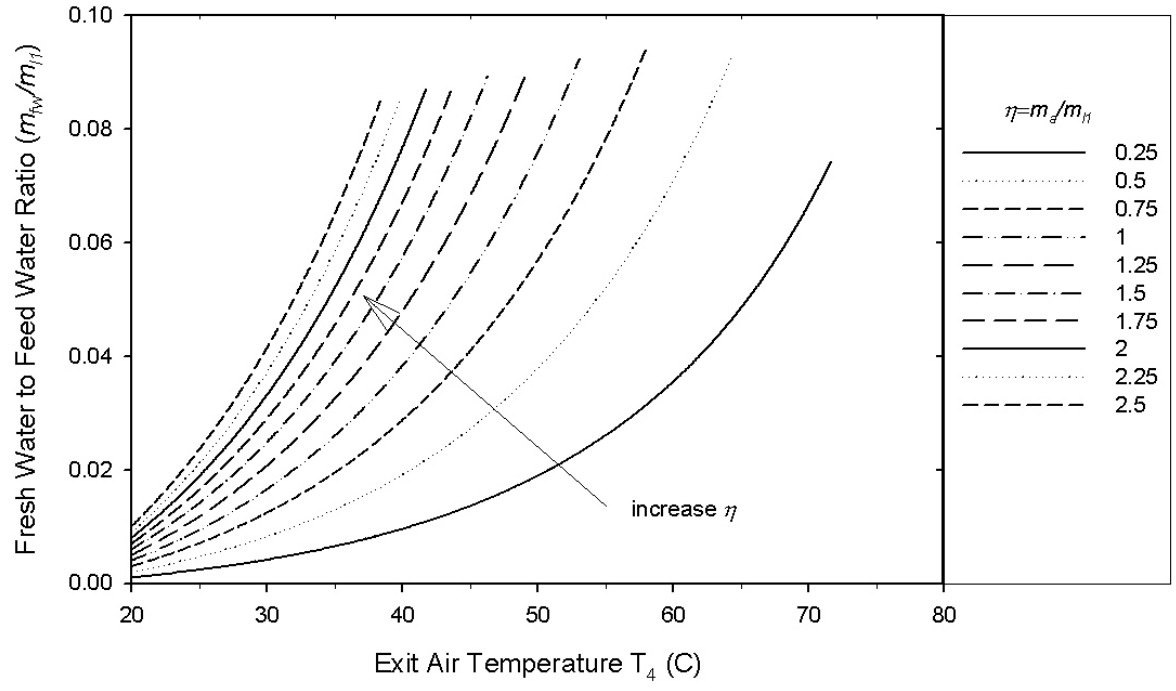

Figure 10 Fresh water production efficiency, T_H=80° C

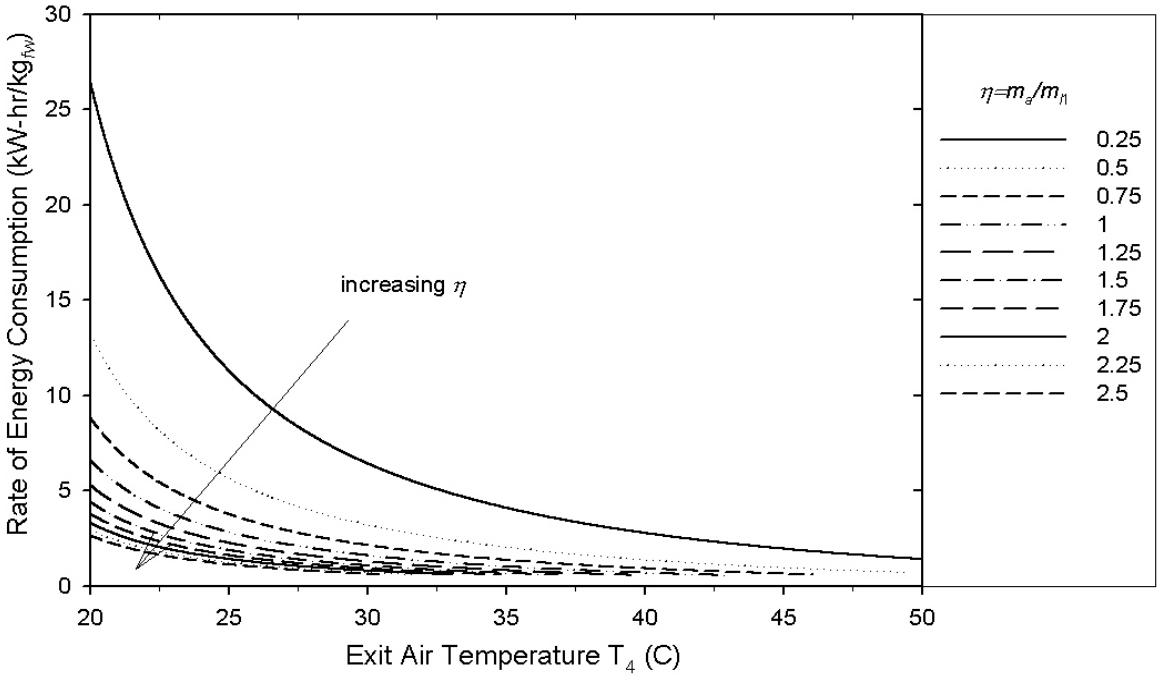

Figure 11 Rate of energy consumption, T_H=50° C

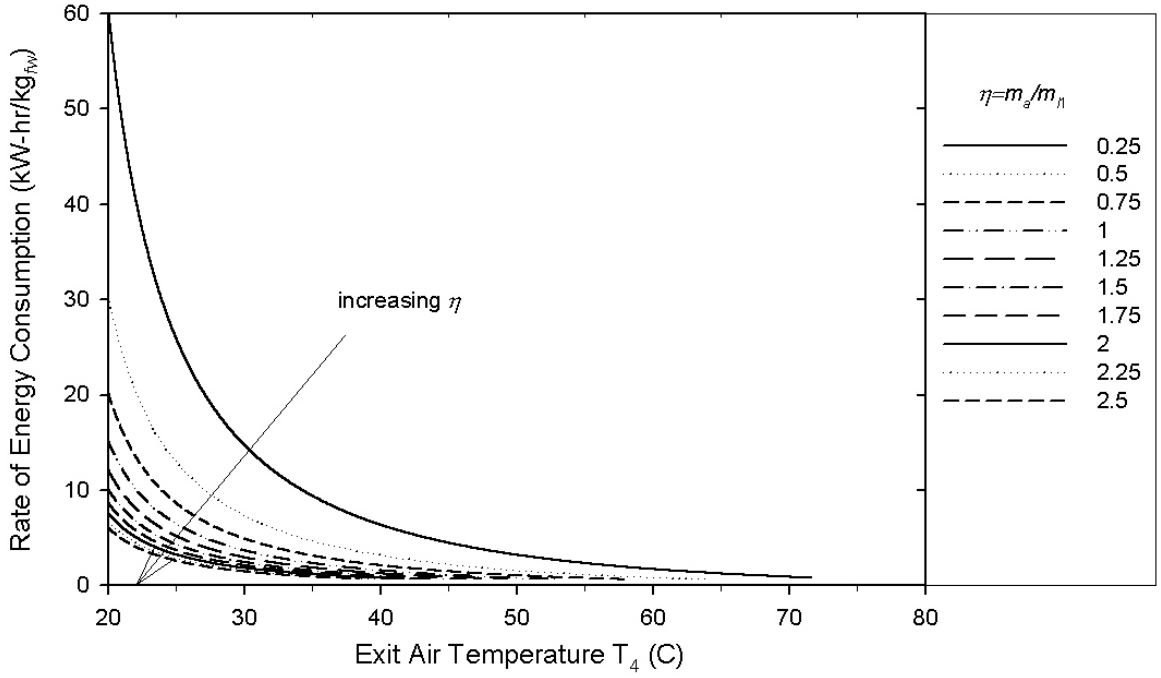

Figure 12 Rate of energy consumption, T_H=80° C

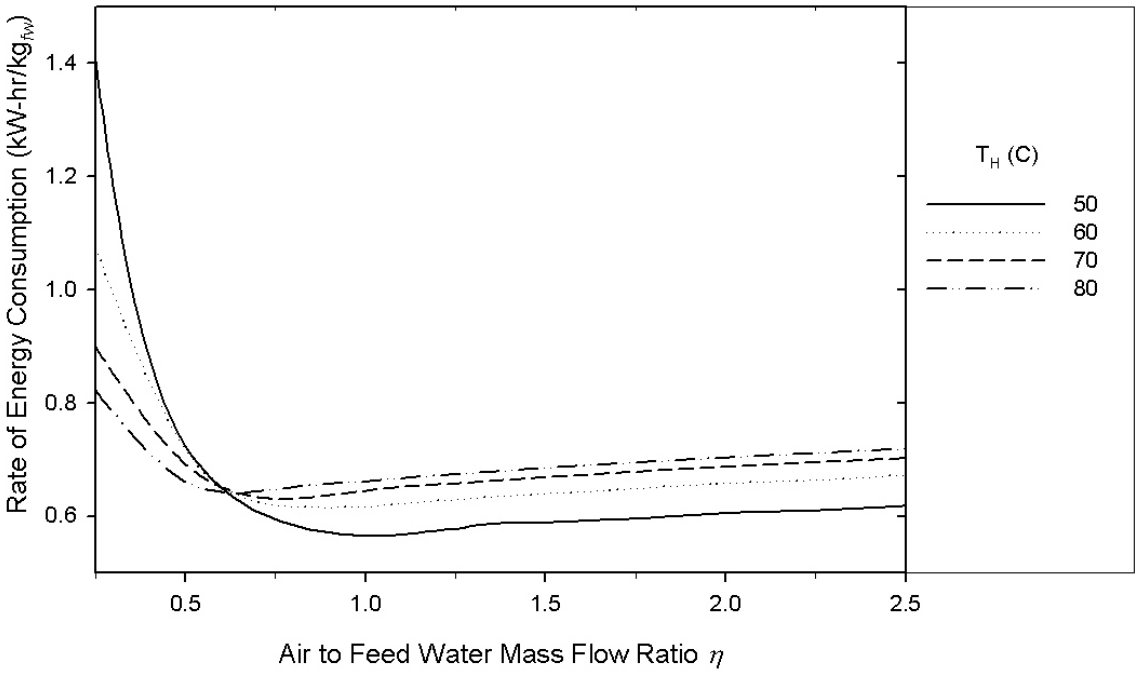

Figure 13 Minimum rate of energy consumption for different T_H

2.1 Application to the Electric Power Industry

The attractive feature of the DDD process is that it can operate at low temperatures so that it requires an energy input with low thermodynamic availability. This is important because the process can be driven by waste heat that would otherwise not be suitable for doing useful work or driving some other distillation process (such as flash distillation). A very interesting application for the DDD process is to operate in conjunction with an existing process that produces large amounts of waste heat and is located in the vicinity of an ocean or sea. One such potential benefactor of the DDD process is the electric utility industry. Conventional steam driven power plants dump a considerable amount of energy to the environment via cooling water that is used to condense low pressure steam within the main condenser. Typically this cooling water is either discharged back to its original source or it is sent to a cooling tower, where the thermal energy is discharged to the atmosphere. Instead of dumping the thermal energy to the environment, the DDD process provides a means for putting the discarded thermal energy to work to produce fresh water. Of course this application is limited to power producing facilities sited along the coastline. However, this should not be a significant limitation. Bullard and Klausner [9] studied the geographical distribution of fossil fired power plants built in the United States from 1970 to 1984. In their study they found that the two most significant attributes for siting a new fossil fired plant in a given geographical region are 1) proximity to a large body of water and 2) proximity to a large population base. The demographic make-up of the United States as well as other industrialized nations is such that major population centers reside along the coastline.

Thus, the DDD process appears to be well suited for the power generation infrastructure in the United States.

As an example, consider that a 100 MW steam driven power plant operating with 2" Hg vacuum in the main condenser would have approximately 140 MW of energy at 93° C available from low pressure condensing steam [10]. If retrofitted with a DDD plant, there is potential to produce as much as 1.51 million gallons of fresh water over a 24 hour period, assuming the feed water temperature enters the diffusion tower at 50° C and 1.44 million gallons of fresh water per day if the feed water temperature is 80° C. The low temperature operation of the DDD process is economically advantageous in that inexpensive materials may be used to construct a facility. Since the energy required to drive the DDD process would be free to an electrical utility, it is anticipated that the capital investment required to fabricate a DDD plant could be readily recovered by selling fresh water to local industry and municipalities. The economic feasibility of the DDD process will ultimately be judged by the operating and capital costs associated with the process.

Another point worth mentioning is that although there exists some optimum air to feed water flow ratio that will minimize the thermal energy consumption, this may not be the most economical operating condition when the DDD process is driven by waste heat. The reason is that a higher air flow rate requires more pumping power, which must be supplied to forced draft fans via electricity. Since electricity is a valuable commodity it may be more economical to operate with a higher exit air temperature and a lower air to feed water flow ratio (lower electricity consumption) since the thermal energy driving the DDD process is waste heat that would otherwise be discarded. An economic analysis, which is not considered here, is required to identify the optimum operating conditions based on cost considerations.

3.0 Diffusion Tower Design, Analysis, and Optimization

The evaporation of mineralized water in the diffusion tower is achieved by spraying heated feed water on top of a packed bed and blowing the dry air concurrently through the bed. The falling liquid will form a thin film over the packing material while in contact with the low humidity ratio turbulent air stream. Heat and mass transfer principles govern the evaporation of the water and the humidification of the air stream. When operating at design conditions, the exit air stream humidity ratio should be as high as possible. The ideal state of the exit air/vapor stream from the diffusion tower is saturated, which is hardly approached in actual practice. The humidified air stream is discharged to a direct contact condenser for fresh water production.

In order to design a DDD plant, it is necessary to size the diffusion tower. Once the size of the diffusion tower is determined, its performance requires determination of the temperature/humidity ratio distribution, energy consumption and fresh water production rate. Therefore a mathematic model has been developed that allows the appropriate size of the diffusion tower to be determined as well as characterize its performance over a series of operating conditions.

The attractive feature of the DDD process is that it can operate at low temperatures so that it requires an energy input with low thermodynamic availability. In

the analyses that will be considered, the process will be driven by waste heat. So the primary energy consumption considered is the electric power required to operate the water pumps and the forced draft blowers, which pump air through the system. Another important target of the computation is to optimize the design of the diffusion tower. There are two optimum conditions that will be considered: minimum energy consumption or maximum fresh water production. The diffusion tower analysis consists of following steps:

1) Identify the desired thermodynamic states of the air and water entering and discharging the diffusion tower;
2) Compute the required height of the diffusion tower for series of specified operating conditions;
3) Compute the pressure drop through the packing material from both the water and gas side;
4) Compute the fresh water production rate and electrical energy consumption for a range of flow and thermal conditions.

The results of the computation will be used to identify the optimal operating conditions. This section gives a detailed description of the diffusion tower modeling, analysis, and results.

3.1 Heat and Mass Transfer Model for the Diffusion Tower

This section describes the heat and mass transfer formulation and solution procedure required to design and optimize the diffusion tower. The most widely used model to compute the heat and mass transfer associated with air/water evaporating systems is, that due to Merkel [11], which is used to analyze cooling towers. However Merkel's analysis contains two restrictive assumptions,

1) On the water side, the mass loss by evaporation of water is negligible and
2) The Lewis number is unity.

Merkel's analysis is known to under-predict the required cooling tower volume and is not useful for current analysis since the purpose of the diffusion tower is to maximize the evaporation of water for desalination. A pictorial view of the diffusion tower is shown in Figure 14.

The current formulation is based on a two-fluid film model in which conservation equations for mass and energy are applied to a differential control volume, also shown in Figure 14. The conservation of mass applied to the liquid phase of the control volume in Fig. 14 results in,

$$\frac{d}{dz}(m_{L,z}) = \frac{d}{dz}(m_{V,evap}), \tag{8}$$

where the subscript evap denotes the portion of liquid evaporated. Likewise, the conservation of mass applied to the gas (air/vapor mixture) side is expressed as,

$$\frac{d}{dz}(m_{V,z}) = \frac{d}{dz}(m_{V,evap}). \tag{9}$$

For an air/water-vapor mixture the humidity ratio may is related to the relative humidity, Φ, through,

$$\omega = \frac{m_V}{m_a} = \frac{0.622\Phi P_{sat}(T_a)}{P - \Phi P_{sat}(T_a)}, \tag{10}$$

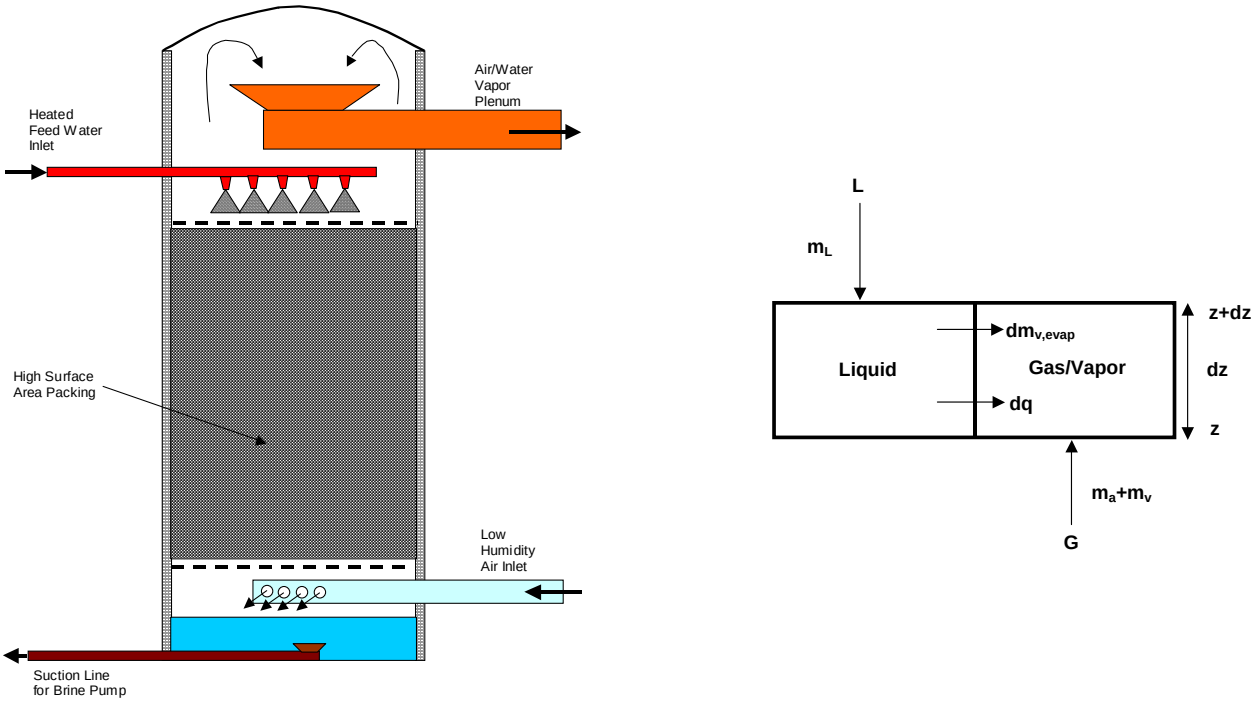

Figure 14 Pictorial view of the diffusion tower and differential control volume for two-fluid model

where P is the total pressure and P_{sat} is the partial pressure of vapor. Using the definition of the mass transfer coefficient applied to the differential control volume, the gradient of the evaporation rate is expressed as,

$$\frac{d}{dz}(m_{V,evap}) = k_G a \frac{M_V}{R}\left(\frac{P_{sat}(T_L)}{T_L} - \frac{\Phi P_{sat}(T_a)}{T_a}\right)A, \qquad \textbf{(11)}$$

where k_G is the mass transfer coefficient on gas side, a is the specific area of the packing material, M_V is the vapor molecular weight, R is the universal gas constant, and A is the cross sectional area of the diffusion tower. Combining Eqs. (9),(10), and (11) the gradient of the humidity ratio in the diffusion tower is expressed as,

$$\frac{d\omega}{dz} = \frac{k_G a}{G}\frac{M_V}{R}\left(\frac{P_{sat}(T_L)}{T_L} - \frac{\omega}{0.622+\omega}\frac{P}{T_a}\right), \qquad \textbf{(12)}$$

where $G = {}^{m_a}\!/_{A}$ is the air mass flux. Equation (12) is a first order ordinary differential equation with dependent variable, ω, and when solved yields the variation of humidity ratio along the length of the diffusion tower.

The conservation of energy applied to the liquid phase of the control volume yields,

$$\frac{d}{dz}(m_L h_L) = \frac{d(m_{V,evap})}{dz} h_{Fg} + Ua(T_L - T_a)A, \quad \textbf{(13)}$$

where U is the overall heat transfer coefficient. Noting that $dh_L = C_{p_L} dT_L$, and combining with Eqs. (13), and (8) results in an expression for the gradient of water temperature in the diffusion tower,

$$\frac{dT_L}{dz} = \frac{m_a}{m_L}\frac{d\omega}{dz}\frac{(h_{Fg} - h_L)}{C_{p_L}} + \frac{Ua(T_L - T_a)}{C_{p_L} L}, \quad \textbf{(14)}$$

where L= m_L / A is the water mass flux. Equation (14) is also a first order ordinary differential equation with T_L being the dependent variable and when solved yields the water temperature distribution through the diffusion tower.

The conservation of energy applied to the air/water-vapor phase of the control volume yields,

$$-\frac{d}{dz}(m_a h_a + m_V h_V) + \frac{d(m_{V,evap})}{dz} h_{Fg} = -Ua(T_L - T_a)A. \quad \textbf{(15)}$$

Noting that the specific heat of the air/vapor mixture is evaluated as

$$C_{p_{mix}} = \frac{m_a}{m_a + m_V} C \quad + \frac{m_V}{m_a + m_V} C_{p_V}, \quad \textbf{(16)}$$

p_a

and combining Eqs. (15) and (9) yields the gradient of air temperature in the diffusion tower,

$$\frac{dT_a}{dz} = -\frac{1}{1+\omega}\frac{d\omega}{dz}\frac{h_L(T_a)}{C_{p_{mix}}} + \frac{Ua(T_L - T_a)}{C_{p_{mix}} G(1+\omega)}, \quad \textbf{(17)}$$

Equation (16) is also a first order ordinary differential equation with T_a being the dependent variable and when solved yields the air/vapor mixture temperature distribution through the diffusion tower.

Equations (12), (14), and (16) comprise a set of coupled ordinary differential equations that are used to solve for the humidity ratio, water temperature, and air/vapor mixture temperature distributions through the diffusion tower. However, since a one-dimensional formulation is used, these equations require closure relationships. Specifically, the overall heat transfer coefficient and the gas side mass transfer coefficient are required. A significant difficulty which has been encountered in this analysis is that correlations for the water and air/vapor heat transfer coefficients for film flow though a packed bed available in the open literature (McAdams et al. [12] and Huang and Fair [13]) are presented in dimensional form. Such correlations are not useful for the present analysis since a special matrix type packing material is utilized. In order to overcome this difficulty the mass transfer coefficients are evaluated for the liquid and gas flow using a reliable correlation and a heat and mass transfer analogy is used to evaluate the heat transfer coefficients.

The mass transfer coefficients associated with film flow in diffusion towers have been widely investigated. The most widely used and perhaps most reliable correlation is that proposed by Onda et al. [14]. Onda's correlation is used to calculate the mass transfer coefficients in the diffusion tower as,

mass transfer coefficient on the liquid side

$$k_L = 0.0051 \mathrm{Re}_{LW}^{2/3} \, Sc_L^{-0.5} (a \cdot d_P)^{0.4} (\frac{\mu_L g}{\rho_L})^{1/3}, \quad \textbf{(18)}$$

mass transfer coefficient on the gas side

$$k_G = 5.23 \mathrm{Re}_{GA}^{0.7} \, Sc_G^{1/3} (a \cdot d_P)^{-2} \, aD_G . \quad \textbf{(19)}$$

In above equations, the dimensionless variables are defined by,

$$a_W = a\left\{1 - \exp[-1.45(\frac{\sigma_c}{\sigma_L})^{3/4} \, \mathrm{Re}_{LA}^{1/10} \, Fr_L^{-0.05} We_L^{1/5}]\right\}, \quad \textbf{(20a)}$$

$$\mathrm{Re}_{LW} = \frac{L}{a_W \mu_L}, \quad \textbf{(20b)}$$

$$\mathrm{Re}_{GA} = \frac{G}{a\mu_G}, \quad \textbf{(20c)}$$

$$\mathrm{Re}_{LA} = \frac{L}{a\mu_L}, \quad \textbf{(20d)}$$

$$Sc_L = \frac{\mu_L}{\rho_L D_L}, \quad \textbf{(20e)}$$

$$Sc_G = \frac{\mu_G}{\rho_G D_G}, \quad \textbf{(20f)}$$

$$Fr_L = \frac{L^2 a}{\rho_L g}, \quad \textbf{(20g)}$$

$$We_L = \frac{L^2}{\rho_L \sigma_L a}, \quad \textbf{(20h)}$$

where d_p denotes the diameter of the packing material, D_L is the molecular diffusion coefficient in liquid, D_G is the molecular diffusion coefficient in air, μ_L is the dynamic viscosity of liquid, μ_G is the dynamic viscosity of air, ρ_G is the density of air, σ_L is the surface tension of liquid, σ_c is the critical surface tension of the packing material.

As mentioned previously, the heat and mass transfer analogy is used to compute the heat transfer coefficients for the liquid side and the gas side. Therefore the heat transfer coefficients are computed as follows,

heat transfer coefficient on the liquid side

$$\frac{Nu_L}{\mathrm{Pr}_L^{1/2}} = \frac{Sh_L}{Sc_L^{1/2}}, \quad \textbf{(21)}$$

$$U_L = k_L (\rho_L C_{PL} \frac{K_L}{D_L})^{1/2}, \quad \textbf{(22)}$$

heat transfer coefficient on the gas side

$$\frac{Nu_G}{\mathrm{Pr}_G^{1/3}} = \frac{Sh_G}{Sc_G^{1/3}}, \quad \textbf{(23)}$$

$$U_G = k_G(\rho_G C_{PG})^{1/3}(\frac{K_G}{D_G})^{2/3}, \quad \textbf{(24)}$$

overall heat transfer coefficient

$$U = (U_L^{-1} + U_G^{-1})^{-1}. \quad \textbf{(25)}$$

When comparing with the data of Huang and Fair (1989) [13] to the predicted heat transfer coefficient on the gas side, the agreement is good, but the liquid side heat transfer coefficient is over-predicted. However, since the gas side heat transfer controls the thermal resistance, the error in the overall heat transfer coefficient is small. The development of a generalized method for predicting the heat transfer through the diffusion tower is an area that deserves further consideration and is the focus of the current experimental investigation.

Eqs. (12), (14), and (16) are simultaneously solved using a fourth order Runge-Kutta marching scheme. The results of the numerical solution are used to evaluate the performance of the diffusion tower for different operating conditions. Once the tower height is calculated, the fresh water production, the water/gas pressure drop through the packing material and the energy consumption rate are computed.

The fresh water production is calculated as,

$$m_f = GA(\omega_{out} - \omega_{in}), \quad \textbf{(26)}$$

where subscripts f, in, and out respectively refer to the fresh water, inlet and outlet.

The pressure drop through the packing material is calculated as,

pressure drop for water

$$\Delta P_L = \rho_L g H, \quad \textbf{(27)}$$

pressure drop for gas/vapor

$$\frac{\Delta P_G}{z} = \frac{G^2}{\rho_G}[0.0354 + 5.05\times10^{-5}(\frac{L}{\rho_L})^2 + 7.0\times10^{-8}(\frac{L}{\rho_L})^4\frac{G^4}{\rho_G^2}] \quad \textbf{(28)}$$

The energy consumption due to pumping water and air through the diffusion tower is calculated from:

rate of energy consumption on the liquid side

$$Pw_L = m_L g H = \frac{LA}{\rho_L}\Delta P_L, \quad \textbf{(29)}$$

rate of energy consumption on the air/vapor side

$$Pw_G = V_G \Delta P_G = \frac{m_G}{\rho_G}\Delta P_g = \frac{GA}{\rho_G}\Delta P_G, \quad \textbf{(30)}$$

total rate of energy consumption

$$Pw = Pw_L + Pw_G, \quad \textbf{(31)}$$

the energy consumption per unit of fresh water production is calculated from:

$$Pw_f = \frac{Pw}{m_f}. \quad \textbf{(32)}$$

In above H denotes the height of the diffusion tower, Pw is the electrical power consumption, V_G is the air/vapor volume flow rate. The pressure drop correlation expressed in Eq. (28) was provided by the manufacturer of the packing material.

For all computations considered in this report, the water inlet temperature, gas inlet humidity ratio, diameter of the diffusion tower, specific area of the packing material and diameter of the packing material are respectively fixed as 50° C, 0.0107, 15 m, 433.1 m^2/m^3 and 0.01m. The inlet water mass flux is varied from 0.5 kg/m^2-s to 10 kg/m^2-s, meanwhile the air to feed water mass flow ratio (m_a/m_{L1}) is varied from 0.3 to 1.5 for every fixed inlet water mass flux. The reason that the inlet feed water temperature is fixed at 50° C is that this is typically the highest water temperature that can be expected to exit the main condenser at a steam power plant.

3.2 Computational analysis

The objective of the computational analysis is to explore the influence of the operating parameters on the diffusion tower performance. These parameters include the water/air/vapor temperatures, humidity ratio, water mass flux, air to feed water mass flow ratio, and tower size. The water mass flux and the air to feed water mass flow ratio through the diffusion tower are two primary controlling variables in the analysis. An experimental facility has been fabricated that will be used to validate the model predictions.

Temperature and humidity variation in the diffusion tower

For a water inlet temperature of 50° C, water mass flux of 5 kg/m^2-s and air to feed water mass flow ratio of 1, the required diffusion tower height is about 0.4 m. Figure 15 shows the computed liquid temperature, air temperature and humidity ratio variation through the diffusion tower. With a mass flux of 5 kg/m^2-s through a 15 m diameter diffusion tower the outlet humidity ratio is approximately 0.055, which corresponds to a fresh water production rate of about 0.9 million gallons per day.

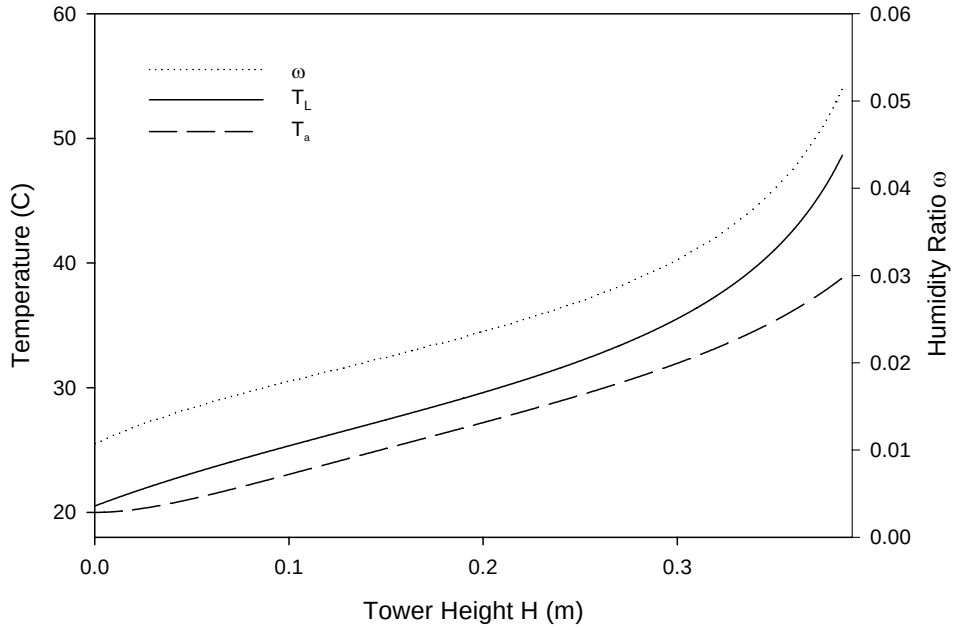

Figure 15 Temperature and humidity ratio profiles through the diffusion tower (5 kg/m^2s inlet water mass flux, 20°C air inlet temperature)

Diffusion tower size

Figure 16 shows the required diffusion tower height for different air to feed water mass flow ratios and varying inlet water mass flux. The tower height is computed such that the maximum possible humidity ratio leaves the diffusion tower. For every fixed air to feed water mass flow ratio, the required diffusion tower height increases with increasing the inlet water mass flux and decreases with increasing air to feed water mass flow ratio.

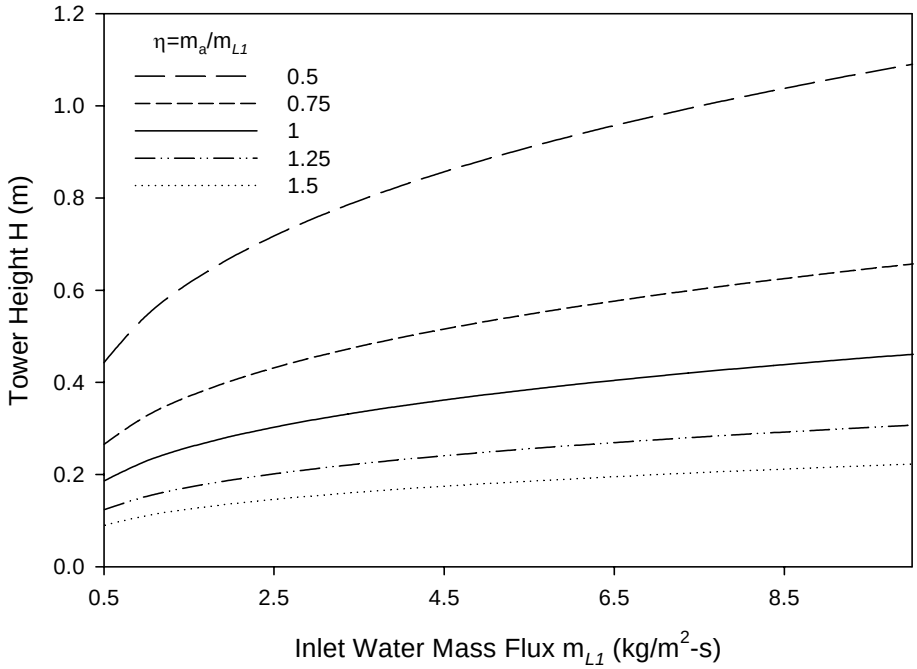

Figure 16 Required tower height variation with inlet water mass flux

Figure 17 shows the required diffusion tower height for different inlet water mass flux and varying air to feed water mass flow ratio. For the same inlet water mass flux, the required diffusion tower height decreases with increasing air to feed water mass flow ratio as is observed in Figure 16.

Figure 16 and 17 clearly show that for a fixed inlet water temperature and the maximum possible exit humidity ratio, the required diffusion tower height is strongly influenced by both the inlet water mass flux and the air to feed water mass flow ratio. It is particularly noteworthy that the maximum required diffusion tower height does not exceed 1.2 meters for the operating conditions considered. This is a very important consideration in evaluating the cost of fabricating a desalination system. Due to the small size of the diffusion tower, it is feasible to manufacture the tower off site and deliver it to the plant site following fabrication. This should significantly lower the cost. In the analysis it was assumed that the tower diameter is 15 m. However, a height to diameter ratio of about 5 is typically desired. If a single tower has a diameter of 5 m, then to have an equivalent flow area, a total of nine diffusion towers would be required to operate in parallel for the DDD process.

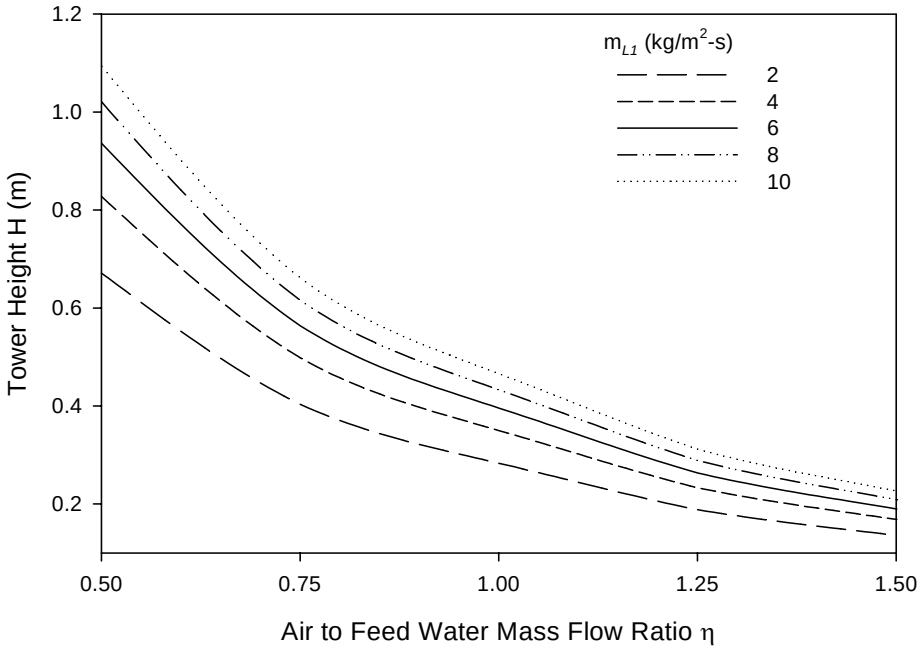

Figure 17 Required tower height variation with air to feed water mass flow ratio

Humidity ratio

Figure 18 shows the maximum possible outlet humidity ratio for different air to feed water mass flow ratios and varying inlet water mass flux. The maximum possible outlet humidity ratio hardly changes with varying inlet water mass flux. However, it shows a strong dependence on the air to feed water mass flow ratio. Figure 19 shows this trend more clearly.

Fig. 18 and Fig. 19 show that for fixed inlet water and air temperatures, the maximum possible outlet humidity ratio is strongly dependent on the air to feed water mass flow ratio and is largely independent of the inlet water mass flux. These results indicate that increasing the air to water mass flow ratio will not necessarily assist in increasing the fresh water production since the exit humidity ratio decreases with increasing air to water mass flow ratio.

Exit air temperature

Figure 20 shows the exit air temperature for different air to feed water mass flow ratios and varying inlet water mass flux. As was the case for the humidity ratio, the exit air temperature is insensitive to variations in the inlet water mass flux, while it highly dependent on the air to feed water mass flow ratio as shown in Figure 21.

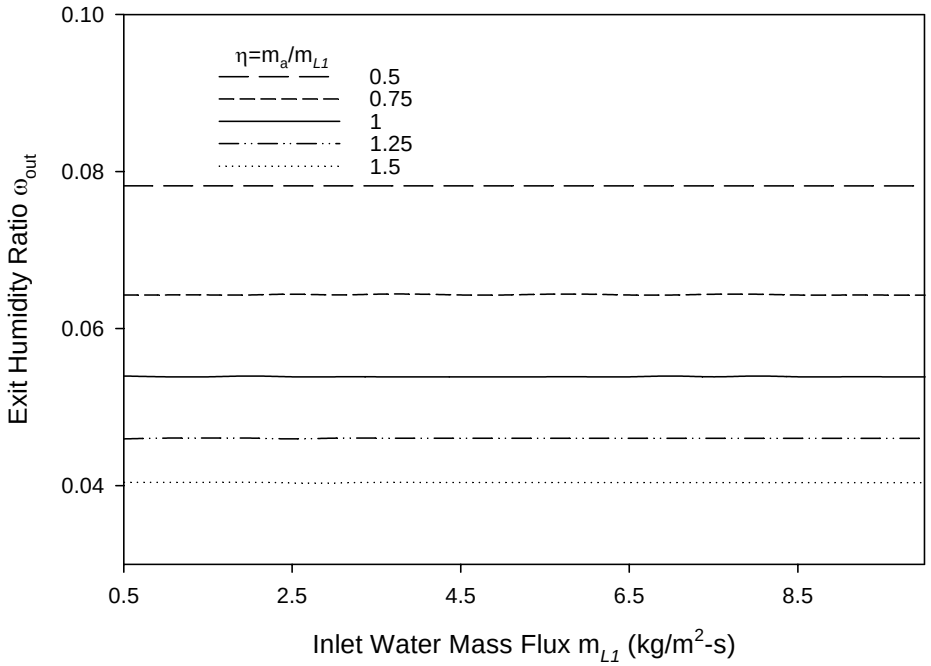

Figure 18 Maximum possible exit humidity ratio with variable inlet water mass flux

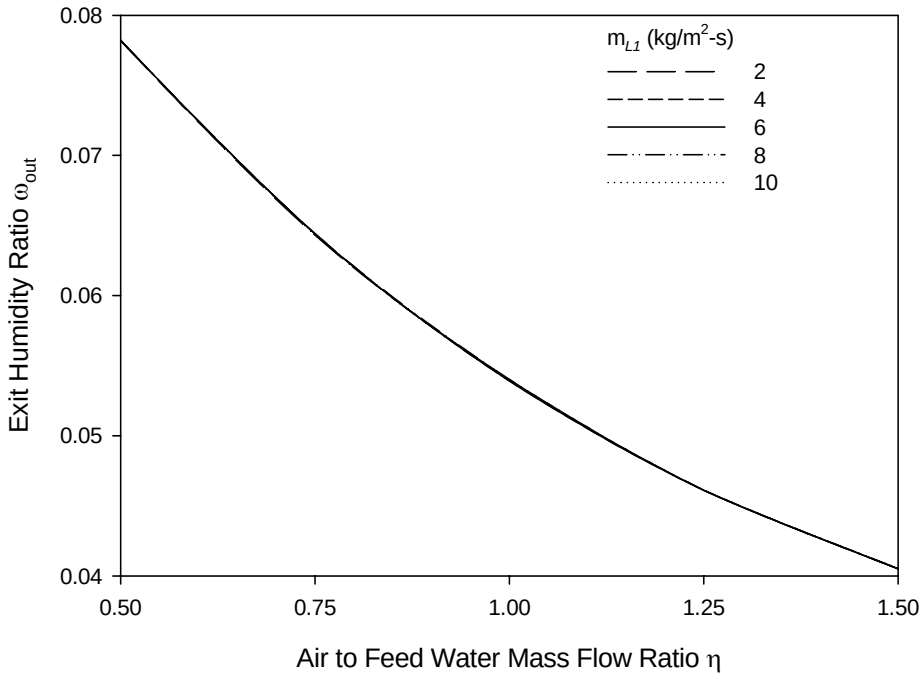

Figure 19 Maximum possible exit humidity ratio for variable air to feed water mass flow ratio

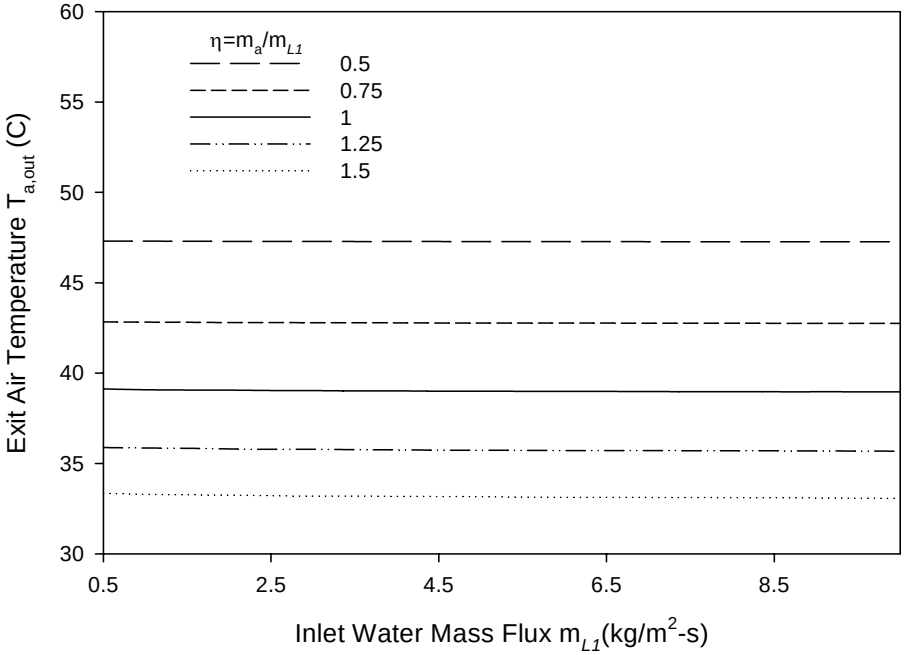

Figure 20 Exit air temperature variation with inlet water mass flux

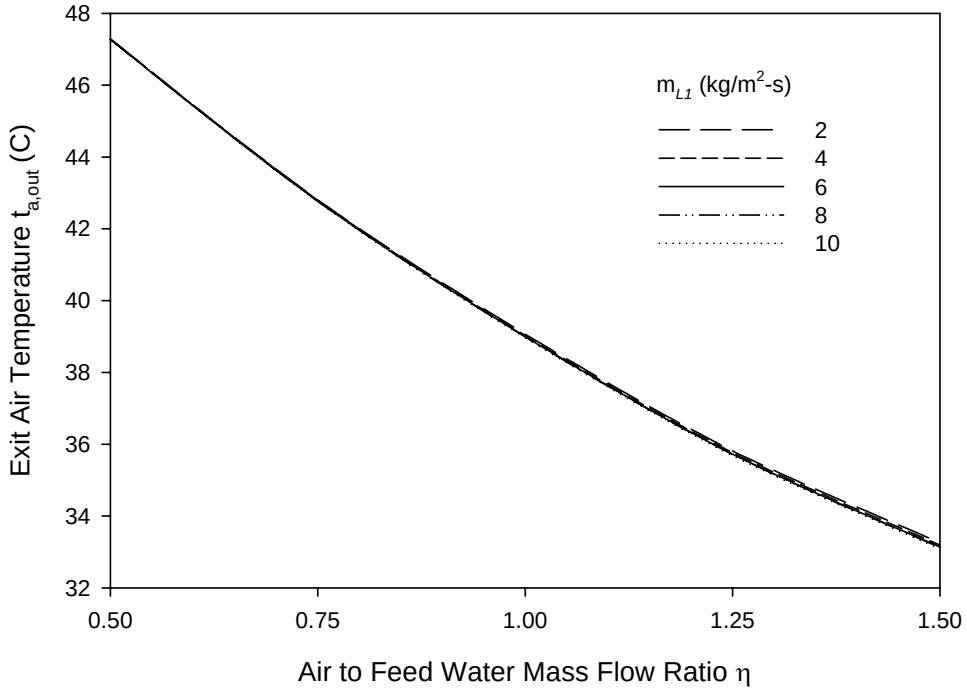

Figure 21 Exit air temperature variation with air to feed water mass flow ratio

Heat and mass transfer coefficients

Figure 22 shows the average gas mass transfer coefficient for different air to feed water mass flow ratios and varying air/vapor mass flux. For the same air to feed water mass flow ratio, the average gas mass transfer coefficient increases with increasing air/vapor mass flux. The gas mass transfer coefficient is insensitive to the air to feed water mass flow ratio.

Figure 23 shows the average overall heat transfer coefficient for different air to feed water mass flow ratios and varying water mass flux. The average overall heat transfer coefficient increases with increasing the water mass flux for a certain air to feed water mass flux; meanwhile, under the same water mass flux, the overall heat transfer coefficient increases with increasing air to feed water mass flow ratio. Examination of Figures 22 and 23 suggests with more water and dry air flowing through the diffusion tower, the heat transfer is more efficient and more fresh water production will be possible. As will be observed this trend holds up to a threshold air to feed water flow ratio, beyond which very little fresh water production is gained.

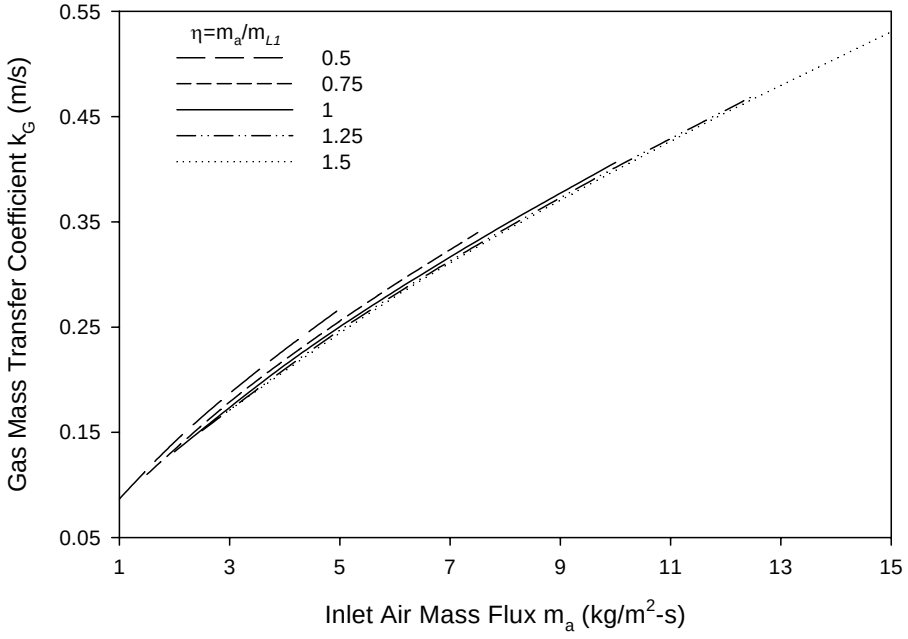

Figure 22 Gas mass transfer coefficient variation with air/vapor mass flux

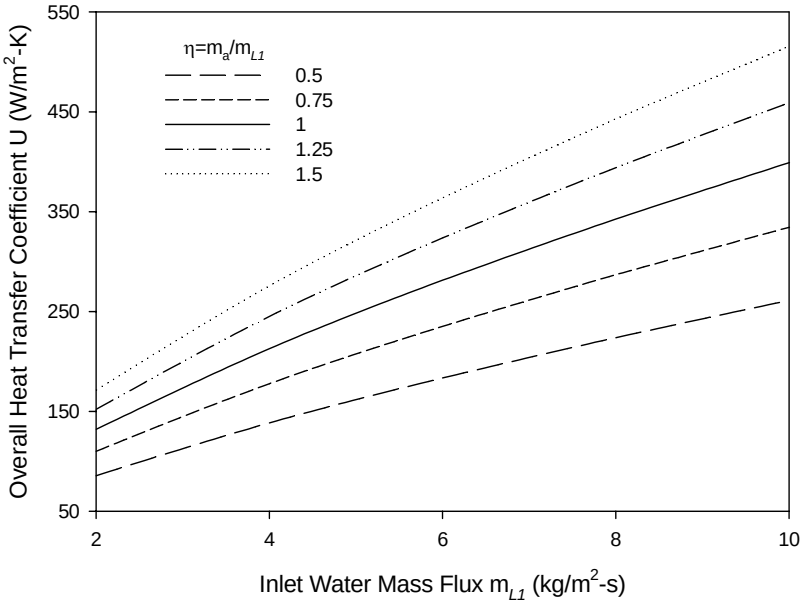

Figure 23 Average overall heat transfer coefficient variation with water mass flux

Fresh water production

Figure 24 shows the fresh water production rate for different air to feed water mass flow ratios with varying inlet water mass flux. At the same air to feed water mass flow ratio, the fresh water production increases almost proportionally with increasing the inlet water mass flux.

Figure 25 shows the fresh water production rate with varying air to feed water mass flow ratio. The fresh water production will initially increase with increasing air to feed water mass flow ratio and tends to be a constant after the air to feed water mass flow ratio exceeds unity. These results clearly indicate that there is nothing to gain in operating with an air to feed water mass flow ratio above unity. Since there is no gain in production it would not make sense to operate with a large air flow rate since it would require larger energy consumption for pumping.

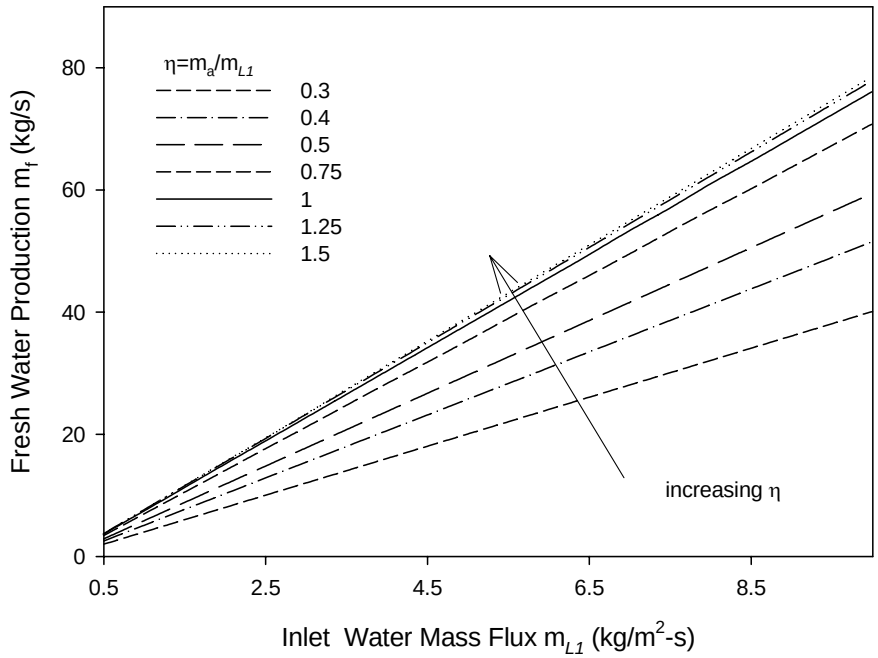

Figure 24 Fresh water production rate variation with inlet water mass flux

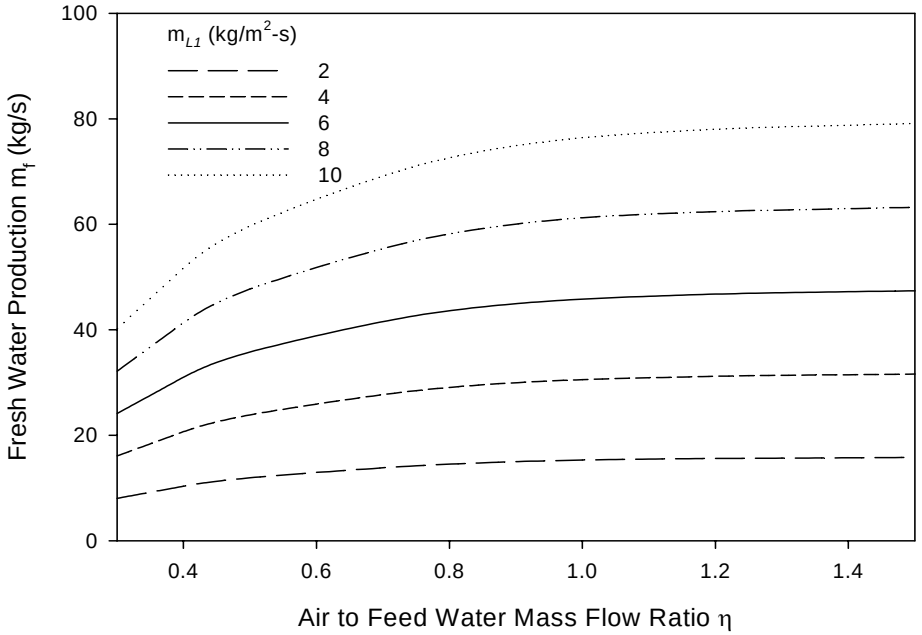

Figure 25 Fresh water production rate variation with air to feed water mass flow ratio

Pressure Drop

Figure 26 shows the water side pressure drop across the diffusion tower for different air to feed water mass flow ratios and varying inlet water mass flux. For a fixed air to feed water mass flow ratio, the water pressure drop increases with the inlet water mass flux. Figure 27 shows the variation of the water side pressure drop with varying air to feed water mass flow ratio. The water pressure drop decreases rapidly with increasing air to feed water mass flow ratio. Figures 26 and 27 illustrate that the water side pressure drop follows the same trend as the diffusion tower height, which is to be expected since the water side pressure drop is due to the gravitational head which must be overcome to pump the water to the top of the diffusion tower.

Figure 29 shows the air side pressure drop in the tower for different air to feed water mass flow ratios and varying inlet water mass flux. With a fixed air to feed water mass flow ratio the air side pressure drop increases rapidly as the inlet water mass flux increases. Figure 30 shows the variation of the air side pressure drop with the air to feed water mass flow ratio. It is observed that there exists a specific air to feed water mass flow ratio that minimizes the air side pressure drop. Also as the air to feed water mass flow ratio exceeds unity, there is not a significant change in the air side pressure drop.

The main energy consumption for the DDD process is due to the pressure loss through the diffusion tower. The total pressure drop is the sum of that on the water side and air side. It is observed that the water side pressure drop is significantly more substantial than that on the air side. However, the pressure drop on the air side is highly dependent on the type of packing material used in the diffusion tower. The low pressure drop observed for the air side is a result of choosing a packing material that has low pressure drop characteristics.

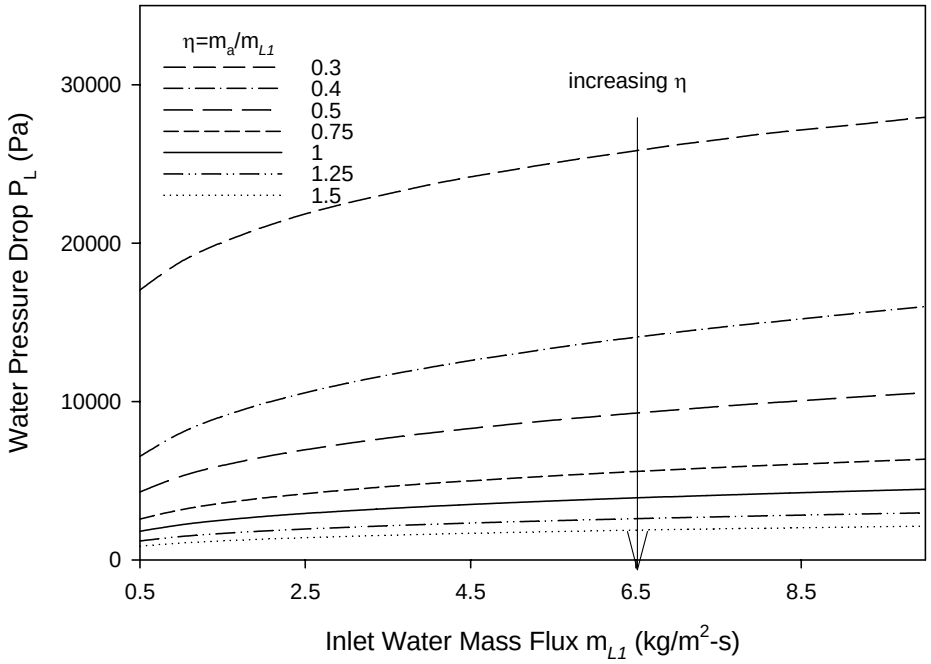

Figure 26 Water side pressure drop variation with inlet water mass flux

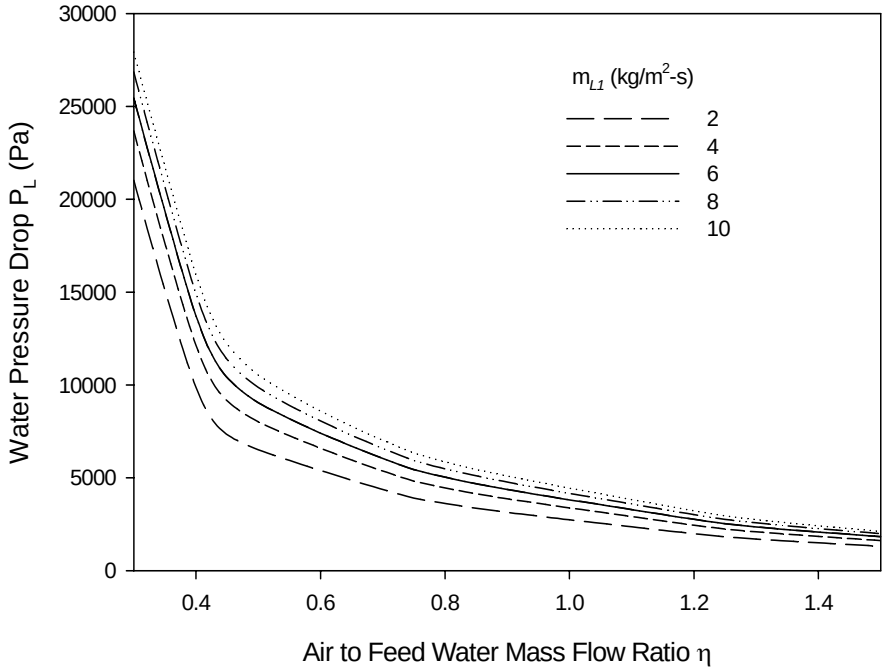

Figure 27 Water side pressure drop variation with air to feed water mass flow ratio

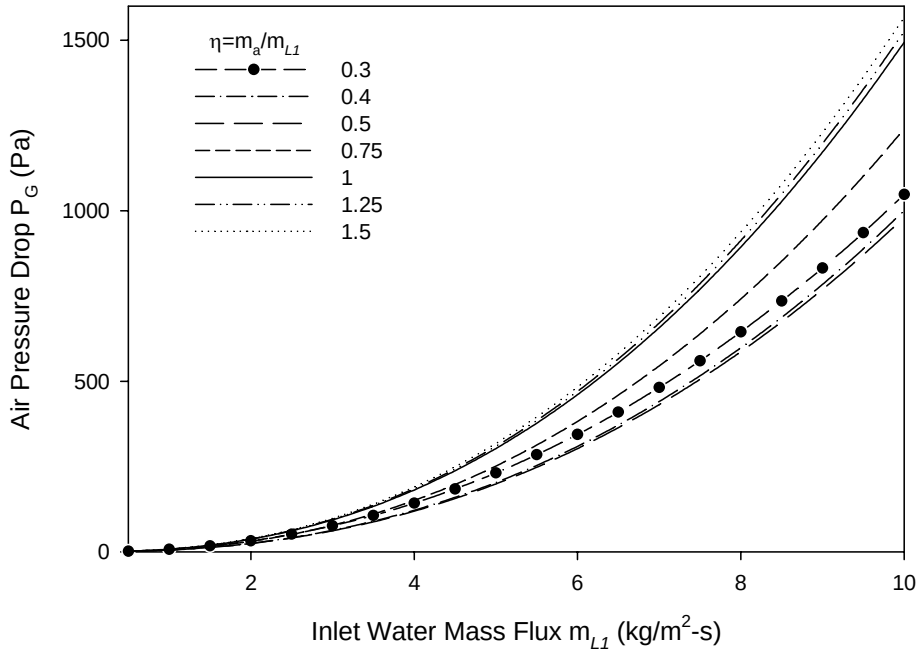

Figure 28 Air/vapor side pressure drop variation with inlet water mass flux

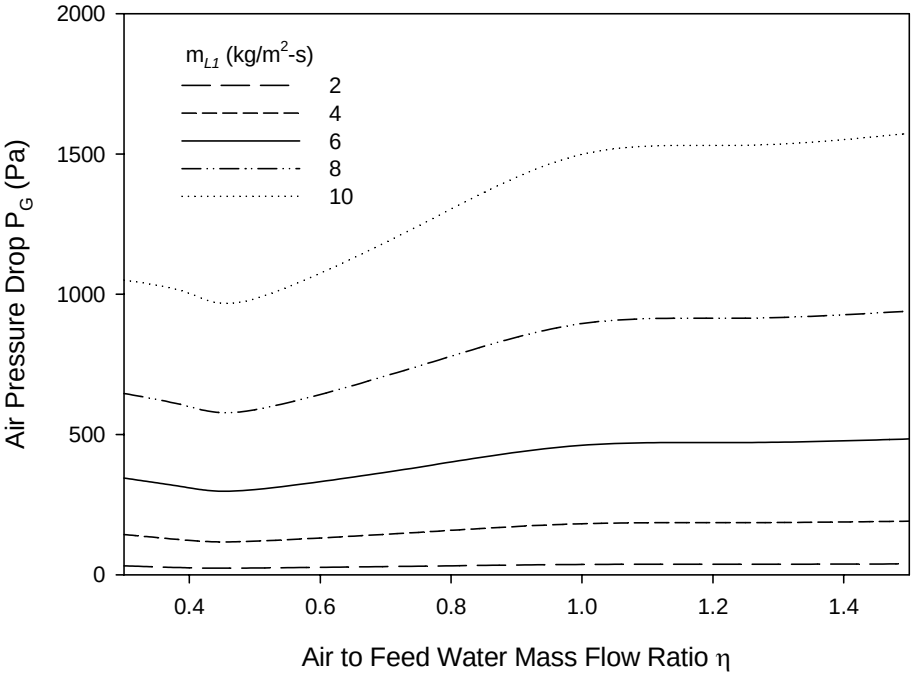

Figure 29 Air/vapor side pressure drop variation with air to feed water mass flow ratio

Energy consumption

Perhaps the most important consideration in this analysis is the rate of energy consumption due to pumping because the operating cost of the DDD process is largely dependent on the cost of electricity to drive the pumps. Figure 30 shows the energy consumption rate for different air to feed water mass flow ratios and varying inlet water mass flux. The energy consumption increases with increasing inlet water mass flux for a fixed air to feed water mass flow ratio. It is particularly interesting that there appears to be a specific air to feed water mass flow ratio that minimizes the energy consumption. This can be observed more clearly in Figure 31, which shows the energy consumption variation with the air to feed water mass flow ratio. There is a minimum energy consumption occurs when the air to feed water mass flow ratio is approximately 0.5. As the inlet water mass flux decreases, the energy consumption becomes relatively insensitive to variations in the air to feed water mass flow ratio.

Optimum design and operating conditions

It is desirable to find a group of suitable operating parameters such as water/air/vapor inlet temperature, inlet humidity ratio, inlet water mass flux and air to feed water mass flow ratio to minimize the diffusion tower energy consumption due to pumping or maximize the fresh water production. Since the water/air/vapor inlet temperature and inlet humidity ratio are decided by the design of the main heater and condenser respectively, it desired is to find a method which can help identify a specific inlet water mass flux coupled with a certain air to feed water mass flow ratio which can minimize the energy consumption for a desired fresh water production rate.

Figure 32 shows the energy consumption rate for different air to feed water mass flow ratios and varying fresh water production rate. The energy consumption increases with increasing production rate, as expected. The energy consumption is minimized when the air to feed water mass flow ratio is 0.5.

Figure 33 shows the energy consumption rate for inlet water mass flux and varying fresh water production level. This Figure again shows that for a fixed inlet water mass flux, the minimum energy consumption occurs when the air to feed water mass flow ratio is 0.5. It also shows that when the air to feed water mass flow ratio exceeds unity, there is no substantial gain in the fresh water production, although the energy consumption increases substantially. This is a very significant observation because it dictates that the air to feed water mass flow ratio should operate between 0.5 and 1. When the air to feed water mass flow ratio is 0.5 the energy consumption in optimized and when it is 1 the fresh water production rate is optimized.

Figure 34 shows the operating conditions that minimize the energy consumption for a desired fresh water production rate. Clearly, the production rate increases with increasing inlet water mass flux. If higher fresh water production rate is desired, there exists an upper limit on the inlet water mass flux beyond which the diffusion tower will flood. Therefore, the present simulation did not consider inlet water mass fluxes beyond 10 kg/m^2-s. Whether or not the diffusion tower will flood is dependent on geometry, inlet water mass flux, inlet air mass flux, and packing material and should be considered in specifying design operating conditions.

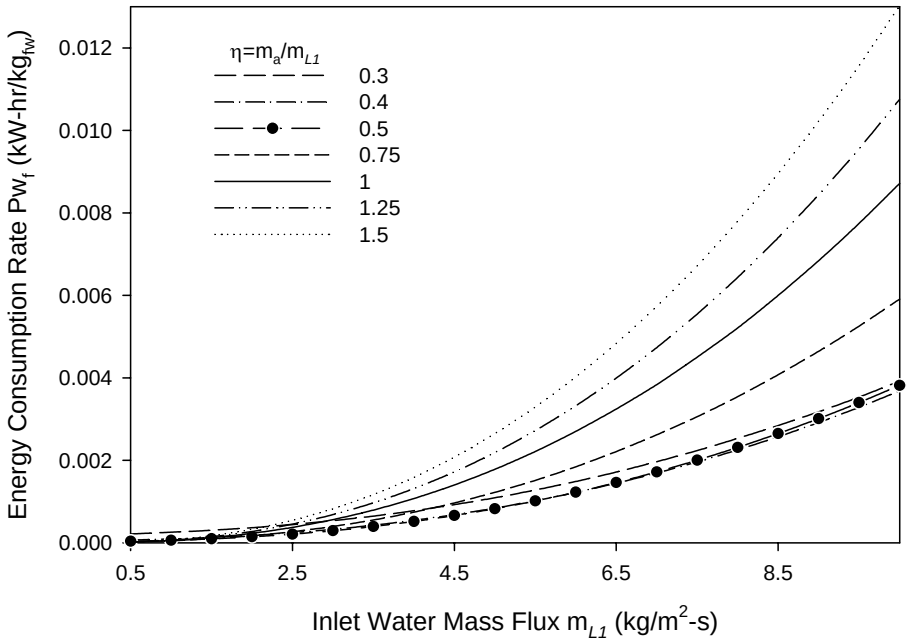

Figure 30 Energy consumption variation with inlet water mass flux

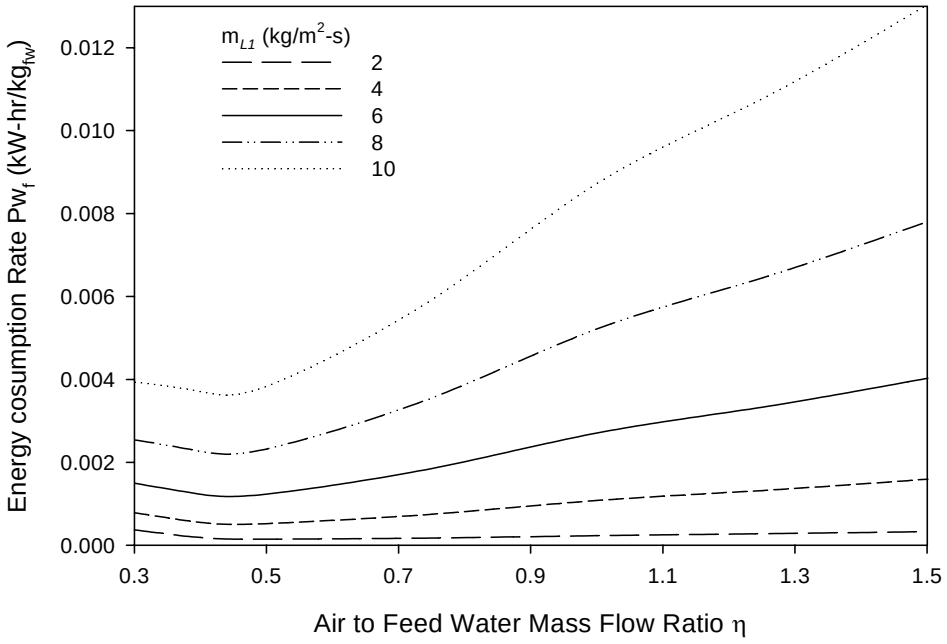

Figure 31 Energy consumption variation with air to feed water mass flow ratio

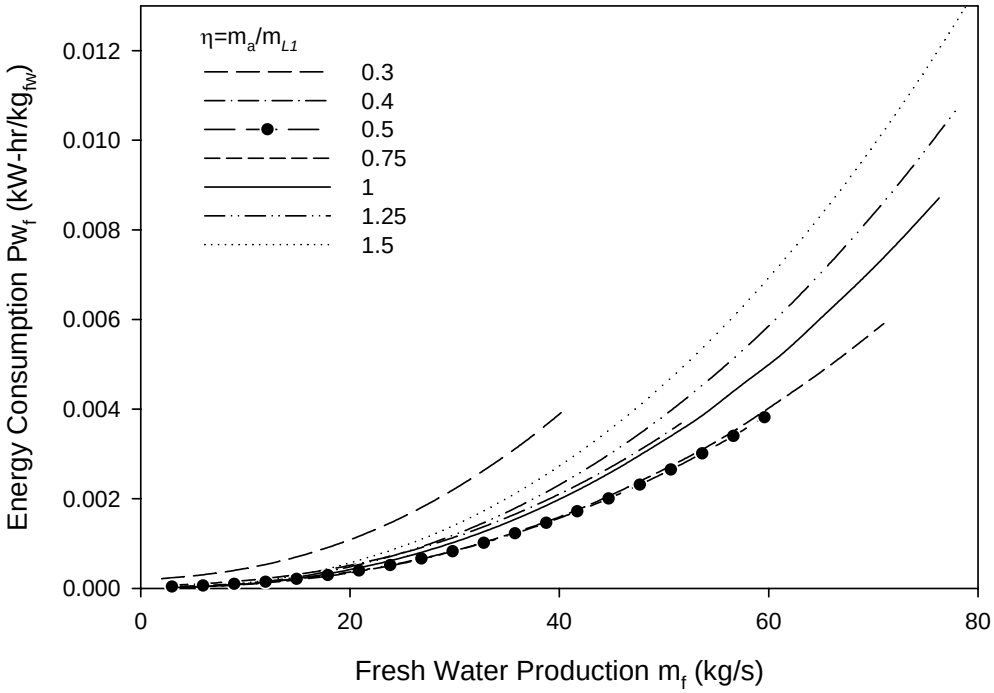

Figure 32 Energy consumption variation with fresh water production at different η

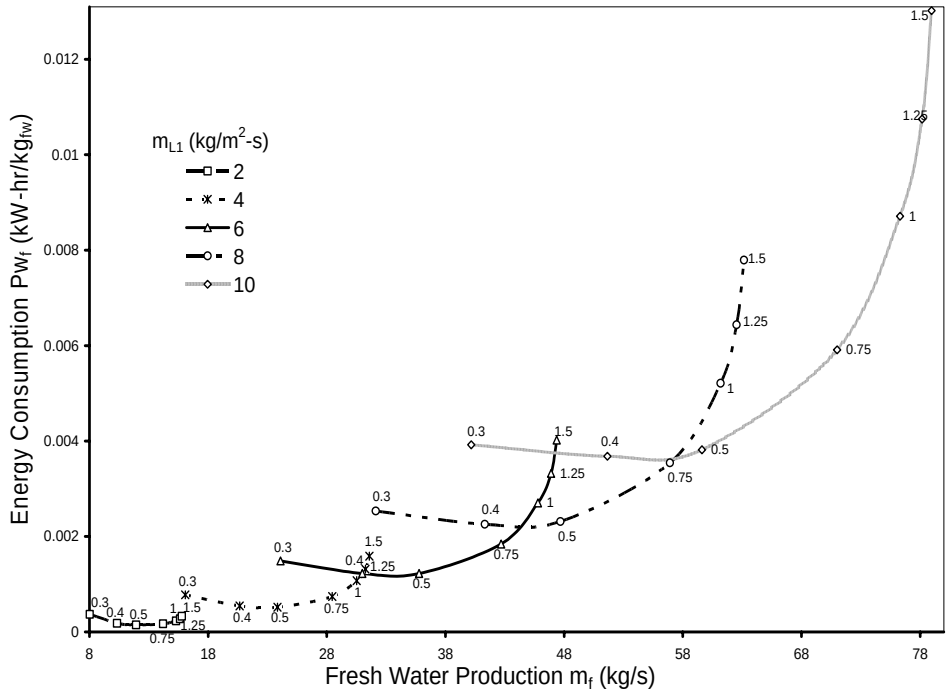

Figure 33 Energy consumption variation with fresh water production for different m_{L1}

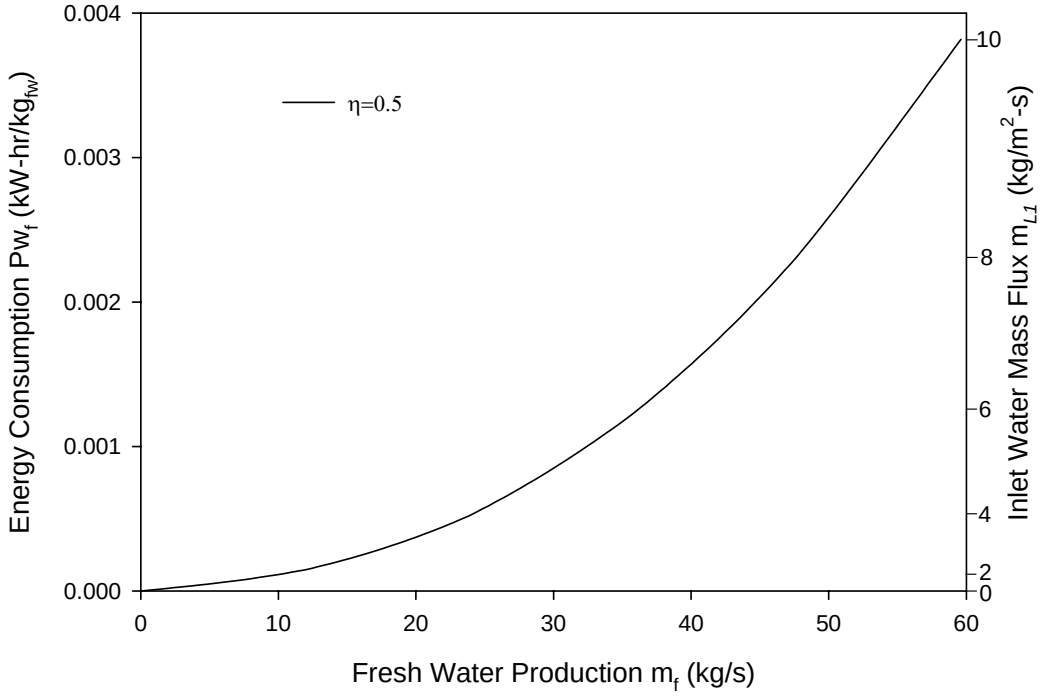

Figure 34 Operating conditions that minimize the energy consumption for a specified for fresh water production rate (50° C water inlet temperature, 20° C air inlet temperature, 15 m equivalent tower diameter)

3.3 Comparison of Diffusion Driven Desalination with multistage flash evaporation and reverse osmosis technologies

In the previous section it was determined that the energy consumption is minimized when the air to water flow ratio is approximately 0.5. For a large production rate (1.5 million gallons per day) the energy consumption is approximately 0.002 kW-hr per kilogram of distilled water. Table 1 below compares the energy consumption of the DDD process with reverse osmosis (RO) and multistage flash evaporation (MSF). It is readily observed that the energy consumption for DDD is about 1/2 of that for RO and an order of magnitude less than that for MSF.

Table 1 Comparison of Energy Consumption for DDD, MSF, and RO Desalination Technologies

Technology	Energy Consumption KW-hr/kg
DDD	0.002
RO	0.005
MSF	0.025

A comparison of the advantages and disadvantages of the DDD, RO, and MSF processes are listed in Table 2. The DDD process is essentially a thermal distillation process that operates using waste heat. It therefore has all of the same operational advantages as MSF. In contrast to MSF, the DDD process has very low energy consumption and thus a low operating cost. The main disadvantage of the DDD process is that the conversion efficiency is low, typically 5-10%. Despite the low conversion efficiency, the energy consumption is still low since pumping occurs at low pressure. However, the low conversion efficiency provides an environmental advantage for the DDD process over RO and MSF. That is the salinity discharge concentration in the brine is comparatively very low. This environmental advantage is a very important issue within North America, Europe, and Japan. For example, the city of Tampa, Florida recently constructed a 25 million gallon per day RO desalination facility. It took over five years to get the environmental permitting to construct the plant, and since its first days of operation there has been growing criticism from environmental groups because of the high salinity discharge concentration into Tampa Bay. The California Coastal Commission recently warned, "desalination could threaten marine life and turn the ocean into a commodity."

Table 2 Comparison of Advantages and Disadvantages of DDD, RO, and MSF Desalination Technologies

Technology	Advantages	Disadvantages
DDD	• Low energy consumption and low cost water production • Waste heat utilized • Low salinity concentration discharge-minimal environmental impact • Low maintenance required	• Lower conversion efficiency
RO	• Feed water does not require heating • Lower energy requirements • Removal of unwanted contaminants such as pesticides and bacteria	• High maintenance required • Performance degrades with time • High salinity concentration discharge-environmental impact • High cost of filter replacement
MSF	• Large production rates and economies of scale • Continuous operation without shutting down	• Large energy consumption • High cost of water production

4.0 Experimental Facility

In previous sections a diffusion driven desalination facility has been described, and its performance has been discussed based on thermodynamic and dynamic transport considerations. In addition, a design and optimization procedure for the diffusion tower performance has been developed. Of course, it is desirable to develop an experimental capability to validate the analytical model of the DDD process and investigate whether the conclusions drawn from the analytical investigation are born out by experiments.

The initial focus of the experimental investigation will be on the diffusion tower. The direct contact condenser will be added to the experimental facility after the performance of the diffusion tower has been thoroughly investigated. The objectives of the first part of the experimental investigation are as follows:

a) Fabricate a laboratory scale diffusion driven desalination facility, including the diffusion tower, up to the direct contact condenser.
b) Instrument the facility sufficiently so that detailed heat and mass transfer measurements may be made as well as measurements of fresh water production and energy consumption.
c) Conduct and array of experiments over the range of parameter space considered in the analysis, and make extensive measurements of heat and mass transfer coefficient, pressure drop, and evaporation rate.
d) Compare the experimental results with the analytical results.
e) Develop a dimensionless correlation for the heat transfer coefficient for air and water flow through packed beds. Make adjustments to analytical model as required.

Figure 35 shows a schematic diagram of the experimental facility. The main feed water is drawn from the municipal water line. The feed water initially passes through a vane type flow meter and then enters a preheater. The preheater is capable of raising the feed water temperature to 50° C. The feedwater then flows through the main heater, which can raise the temperature to saturated conditions. The feedwater temperature is controlled with a PID feedback temperature controller, where the water temperature is measured at the outlet of the main heater. The feed water is then sent to the top of the diffusion tower, where it is sprayed over the top of the packing material.

Dry air is drawn into a centrifugal blower equipped with a 1.5 horsepower motor. The discharge air from the blower flows through a 10.16 cm duct in which a thermal mass flow meter is inserted. The airflow rate is controlled by varying the speed of the blower. A three-phase autotransformer is used to control the voltage to the motor and regulate the speed. Downstream of the thermal mass flow meter the temperature and inlet relative humidity of the air are measured with a thermocouple and a resistance type humidity gauge. The air is forced through the packing material in the diffusion tower and discharges through a plenum and vent at the top of the diffusion tower. At the diffusion tower outlet, the temperature and humidity of the discharge air are measured in the same manner as at the inlet.

The water sprayed on top of the packing material gravitates toward the bottom. The portion of water not evaporated is collected at the bottom of the diffusion tower in a sump

and discharged through a drain. The temperature of the discharge water is measured with a thermocouple. Strain gauge type pressure transducers are mounted at the bottom and top of the diffusion tower to measure the static pressure. A magnetic reluctance differential pressure transducer is used to measure the pressure drop across the length of the packing material.

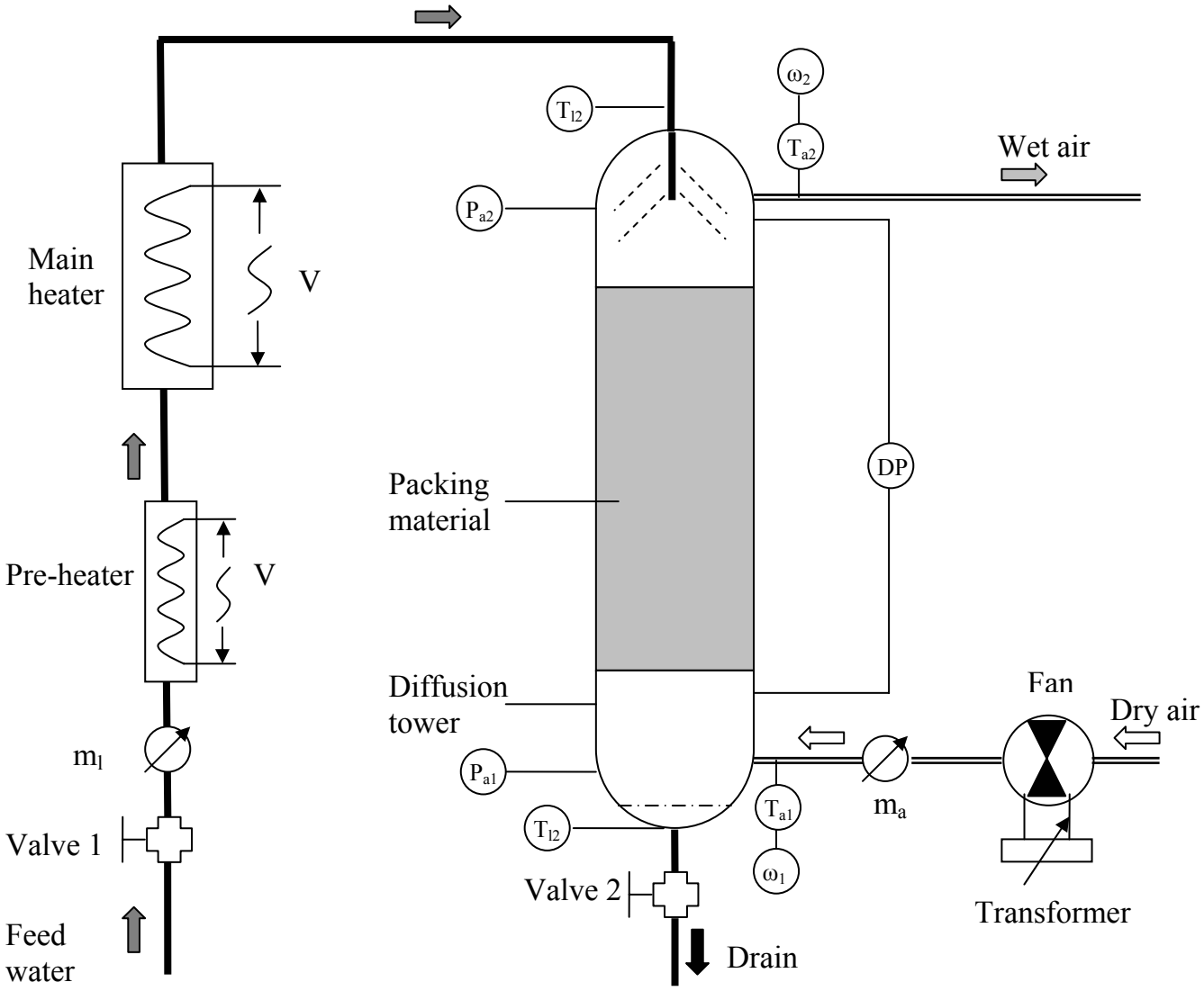

Figure 35 Schematic diagram of DDD facility, with diffusion tower

4.1 Description of Individual Components

Diffusion Tower

A rendered view of the diffusion tower is shown in Figure 36 and a schematic view is shown in Figure 37. The diffusion tower consists of three individual parts: a top chamber containing the air plenum and spray distributor, the main body containing the packing material, and the bottom chamber containing the air distributor and water drain. The top and bottom chambers are constructed from 25.4 cm (10" nominal) ID PVC pipe and the main body is constructed from 24.1 cm ID acrylic tubing with wall thickness of 0.635 cm. The three sections are connected via PVC bolted flanges. The transparent main body accommodates up to 1 m of packing material along the length.

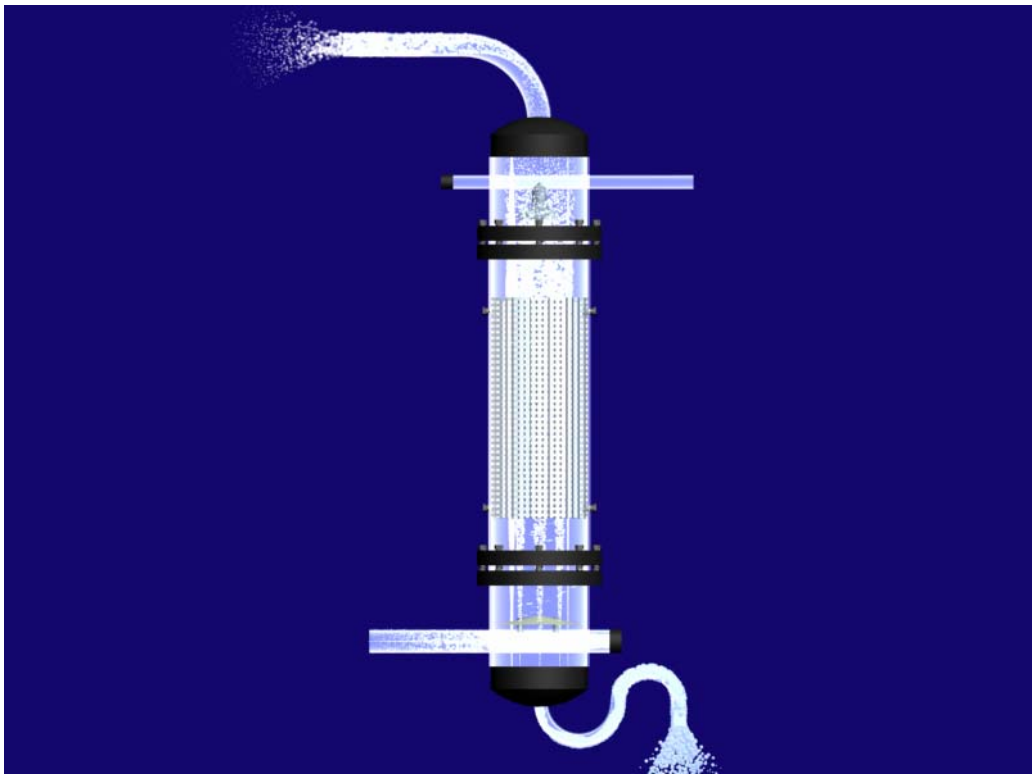

Figure 36 Rendered view of the experimental diffusion tower

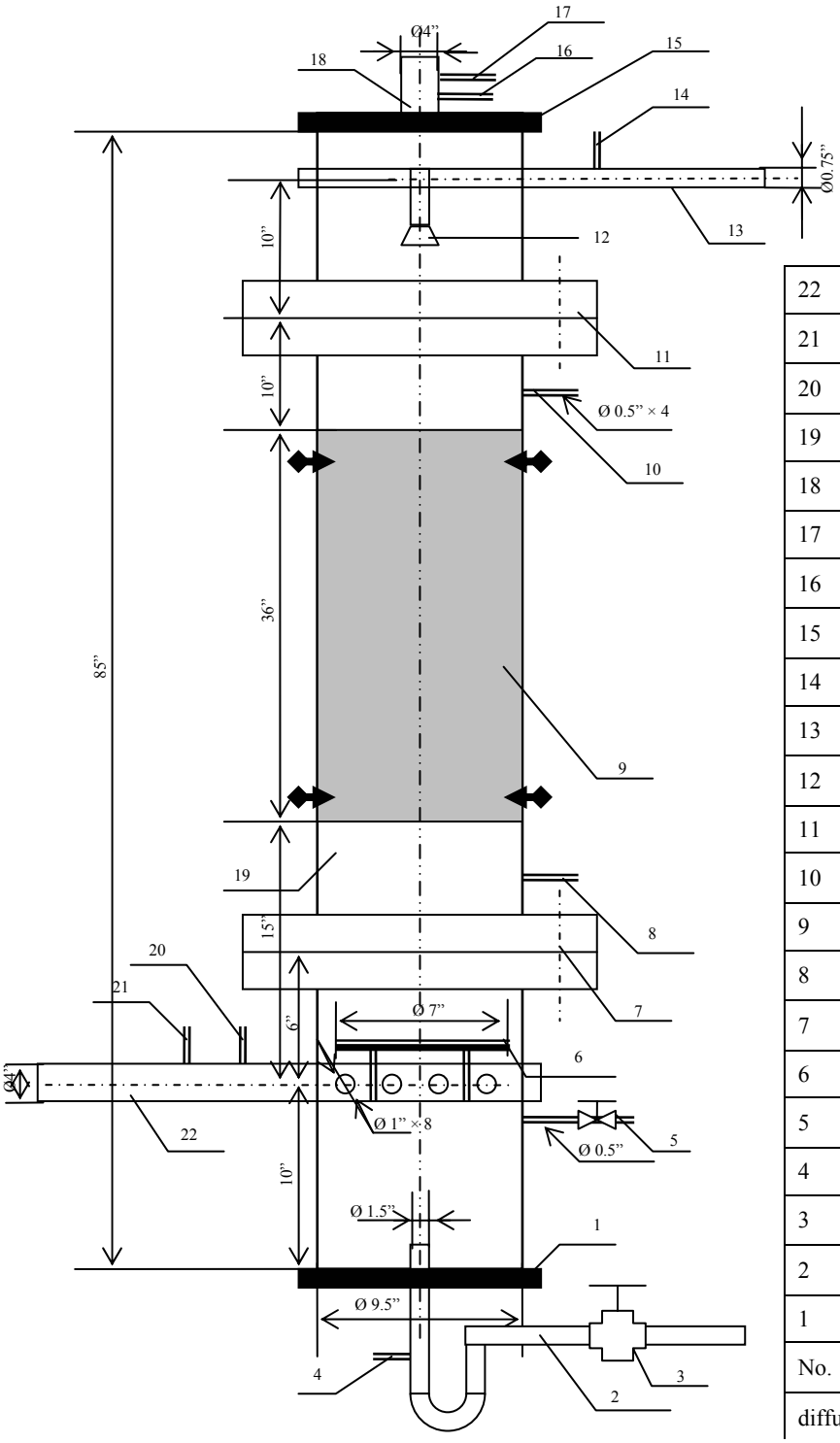

22	gas inlet pipe
21	T_{a1} test pipe
20	ω_1 test pipe
19	diffusion tower
18	gas outlet pipe
17	T_{a2} test pipe
16	ω_2 test pipe
15	top hatch
14	T_{l1} test pipe
13	water inlet pipe
12	sprays
11	top flanges
10	P_{a2} and DP test pipe
9	packing materials
8	P_{a1} and DP test pipe
7	bottom flanges
6	water plate
5	alert pipe
4	T_{l2} test pipe
3	drain valve
2	water outlet pipe
1	bottom hatch
No.	Name
diffusion tower design	

Figure 37 Schematic diagram of experimental diffusion tower

Water Distributor

The water distributor consists of a full cone standard spray nozzle manufactured by Allspray, which maintains a uniform cone angle of 90°. The nozzle is designed to allow a water capacity of about 14.7 LPM, and it's placed more than 50 cm away from the packing material to ensure that the spray covers the whole area. The spray nozzle pictured in Figure 38 is of one-piece construction machined from brass bar stock.

Figure 38 Pictorial view of spray nozzle

Pre-heater

The pre-heater used for the present experiment is 240 V point source water heater. It possesses a self-contained temperature controller and can deliver water outlet temperatures ranging from 30° to 50° C.

Main Heater

The main heater consists of two 3 kW electric coil heaters wrapped around a copper pipe, through which the feed water flows. The power to the heaters is controlled with two PID feedback temperature controllers with a 240 V output. The feedback temperature to the controllers is supplied with a type J thermocouple inserted in the feed water flow at the discharge of the heater.

Packing Material

The packing material to be used for the initial experiments is HD Q-PAC manufactured by Lantec and shown pictorially in Figure 39. The HD Q-PAC, constructed from polyethylene, was specially cut using a hotwire so that it snugly fits into

the main body of the diffusion tower. The specific area of the packing is 433.0709 m^2/m^3 and its effective diameter is 0.01m.

Figure 39 Pictorial view of packing matrix

Water Mass Flow Meter

The vane-type water mass flow meter, constructed by Erdco Corporation, has a range from 1.5-15.14 LPM. It has been calibrated using the catch and weigh method. The flow meter has a 4 to 20 mA output that is proportional to flow rate, and the uncertainty is ± 1% of the full scale. A calibration of the flow meter is shown in Figure 40.

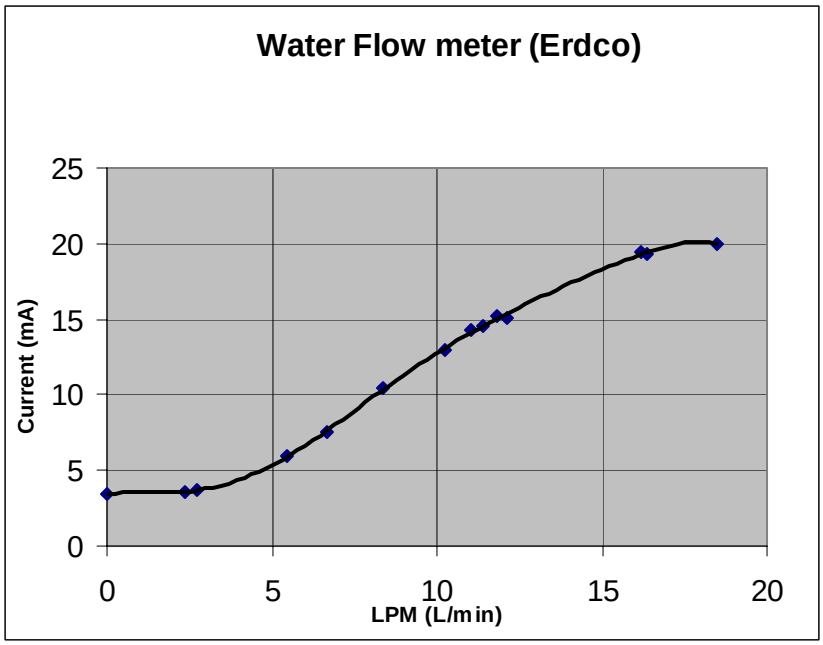

Figure 40 Water Flow meter calibration

Air Mass Flow Meter

The air mass flow rate is measured with a model 620S smart insertion thermal mass flow meter. The flow meter has a response time of 200 ms with changes in mass flow rate. The mass flow meter has a microprocessor-based transmitter that provides a 0-10 V output signal. The mass flow meter electronics are mounted in a NEMA 4X housing. The meter range is 0-1125 SCFM of air at 25°C and 14 PSIG. The uncertainty of the flow meter is ± 1% Full scale + 0.5 % Reading.

Relative Humidity

The relative humidity is measured with two duct-mounted HMD70Y resistance-type humidity and temperature transmitters manufactured by Vaisala Corp. The humidity and temperature transmitters have a 0-10 V output signal and have been factory calibrated.

Temperature and Pressure

All temperature measurements used in the thermal analysis are measured with type E thermocouples. The pressures at the inlet and exit of the diffusion tower are measured with two Validyne P2 static pressure transducers. All of the wetted parts are constructed with stainless steel. The transducers have an operating range from 0-5 psi and have a 0-5 VDC proportional output. The transducers have an accuracy of 0.25% of full scale. They are shock resistant and operate in environments ranging in temperature from –20° to 80° C.

The pressure drop across the test section is measured with a DP15 magnetic reluctance differential pressure transducer. The pressure transducer signal is conditioned with a Validyne carrier demodulator. The carrier demodulator produces a 0-10 VDC output signal that is proportional to the differential pressure. The measurement uncertainty is ±0.25% of full scale.

Data Collection Facility

A digital data acquisition facility has been developed for measuring the output of the instrumentation on the experimental facility. The data acquisition system consists of a 16-bit analog to digital converter and a multiplexer card with programmable gain manufactured by Computer Boards calibrated for type J thermocouples and 0-10V input ranges. A software package, SoftWIRE, which operates in conjunction with MS Visual Basic, allows a user defined graphical interface to be specified specifically for the experiment. SoftWIRE also allows the data to be immediately sent to an Excel spreadsheet.

Ion Chromatograph

One objective of the experimental facility is to quantify the purity of fresh water produced with the DDD facility. For this purpose a Dionex ICS-90 isochromatic ion chromatograph has been installed in the Multiphase Heat Transfer and Fluid Dynamics laboratory. The ICS-90 is capable of measuring mineral concentrations down to several parts per billion.

An assembled view of the diffusion tower is shown in Figure 41. A considerable amount of effort has been put forth in calibrating instrumentation and integrating it with the data acquisition facility. Experimental testing has been initiated, and it is anticipated that extensive measurements of the heat and mass transfer coefficients within the diffusion tower will be collected within the next couple of months.

Figure 41 Assembled View of Diffusion Tower

5.0 Completed Tasks

The following project tasks have been completed:

1.1 Design and fabricate lab scale diffusion tower
1.3 Assemble DDD facilities
1.4 Instrument DDD facilities
4.1 Develop a numerical simulation tool for predicting heat, mass, and momentum transfer in diffusion tower
4.2 Incorporate results from dynamic simulation into a thermodynamic heat and mass balance to predict overall system performance
4.3 Use numerical tools to investigate optimum design criteria and operating conditions

It was anticipated that heat and mass transfer experiments within the diffusion tower would have been initiated at this point in the project. However, unanticipated difficulties in acquiring certain instrumentation have slowed the progress. Other than these difficulties the project has been on schedule. It is anticipated that rapid progress in acquiring heat and mass transfer data can be made and the schedule will fall back on track.

6.0 Summary

The first year progress for the development of a Diffusion Driven Desalination facility has been completed, and the results are promising. A detailed analysis shows that the waste heat from a 1 MW power plant can be used to produce 1.5 million gallons of fresh water per day using the DDD process. The energy used to drive the process is low thermodynamic availability waste heat, and the only energy cost is that used to power the pumps and fans. A simulation of the diffusion tower shows that the pumping power consumption is very competitive compared with the energy costs required for reverse osmosis or flash evaporation technologies. A laboratory scale DDD facility, which includes the diffusion tower, has been fabricated. The direct contact condenser will be added to the facility during next year's investigation. The diffusion tower has been fully instrumented for detailed heat and mass transfer measurements. Extensive measurements will be made during to following year and will be used to validate the simulation.

7.0 References

[1] *Seawater Desalination in California*, 1999, a report by the California Coastal Commission.

[2] Bourouni, K., M. Chaibi, M.T., and Tadrist, L., 2001, **"**Water desalination by humidification and dehumidification of air: State of the art," *Desalination,* Vol. 137, Issues 1-3, pp. 167-176.

[3] Al-Hallaj, S., Farid, M.M., and Tamimi, A.R., 1998, "Solar desalination with a humidification-dehumidification cycle: performance of the unit," *Desalination*, Vol. 120, Issue 3, pp. 273-280.

[4] Assouad, Y., and Lavan, Z., 1988, **"**Solar desalination with latent heat recovery," *Journal of Solar Energy Engineering,* Vol. 110, Issue 1, pp. 14-16.

[5] Larson, R.L., Albers, W., Beckman, J., and Freeman, S., 1989, "The carrier-gas process – a new desalination and concentration technology, *Desalination*, Vol. 73, pp. 119-137.

[6] Al-Hallaj, S., Selman, J.R., *A comprehensive study of solar desalination with a humidification – dehumidification cycle*, 2002, a report by the Middle East Desalination Research Center, Muscat, Sultanate of Oman.

[7] Bharathan, D., Parsons, B.K., and Althof, J.A., 1988, "Direct-Contact Condensers for Open-Cycle OTEC Applications," *National Renewable Energy Laboratory Report SERI/TP-252-3108* for DOE Contract No. DE-AC02-83CH10093.

[8] Bharathan, D., Parent, A., and Hassani, A. V., 1999, "Method and Apparatus for High-Efficiency Direct Contact Condensation," U.S. Patent 5,925,291.

[9] Bullard, C.W. and Klausner, J.F., 1987, "Empirical Analysis of Power Plant Siting," *Energy Systems and Policy*, Vol. 11, pp. 103-120.

[10] El-Wakil, M.M., 1984, *Power Plant Technology*, McGraw-Hill, New York, p. 228.

[11] Merkel, F., 1925, "Verdunstungskuhlung," VDI Forschungsarbeiten, 275, Berlin.

[12] McAdams, W.H., Pohlenz, J.B., and St. John, R.C., 1949, "Transfer of Heat and Mass Transfer Between Air and Water in a Packed Tower," Chemical Engineering Progress, 45, pp. 241-252.

[13] Huang, C.C., and Fair, J.R., 1989, "Direct-Contact Gas-Liquid Heat Transfer in a Packed Column," Heat Transfer Engineering, 10, No. 2, pp. 19-28

[14] Onda, K., Takechi, H, and Okumoto, Y., 1968, "Mass Transfer Coefficients Between Gas and Liquid Phases in Packed Columns," J. Chem. Eng. of Japan, 1, pp. 56-62.

8.0 Nomenclature

A	control surface area (m^2)
a	specific area of packing material (m^2/m^3)
C_{pa}	specific heat of air (kJ/kg)
D	molecular diffusion coefficient (m^2/s)
dp	diameter of the packing material (m)
G	air mass flux (kg/m^2-s)
H	diffusion tower height (m)
h	enthalpy (kJ/kg)
h_{fg}	latent heat of vaporization (kJ/kg)
k_G	mass transfer coefficient (m/s)
L	water mass flux (kg/m^2-s)
M_V	vapor molecular weight (kg/kmol)
m_{l1}	feed water mass flow rate (kg/s)
m_a	air mass flow rate (kg/s)
P_a	partial pressure of air (Pa or kPa)
P_{sat}	partial pressure of vapor (Pa or kPa)
P_w	electrical power consumption (W or kW)
R	universal gas constant (kJ/kmol-K)
R_a	engineering gas constant for air (kJ/kg-K)
$\dot{s}$	entropy generation rate in the diffusion tower (kW/K)
T	temperature (°C or °K)
U	heat transfer coefficient (W/m^2-K)
V	control volume (m^3)
V_G	air/vapor volume flow rate (m^3/s)
Φ	relative humidity
ω	humidity ratio
μ	dynamic viscosity (kg/m-s)
ρ	density (kg/m^3)
σ_L	surface tension of liquid (N/m)
σ_C	critical surface tension of the packing material (N/m)

Subscripts

a	air
evap	the portion of liquid evaporated
fw	fresh water
l	water in liquid phase
v	water in vapor phase
in	inlet parameter
out	exit parameter